Published: 01 March 2007

ARTICLE

Graph evolution: Densification and shrinking diameters

JURE LESKOVEC, Carnegie Mellon University, Pittsburgh, PA, United States

JON MICHAEL KLEINBERG, Cornell University, Ithaca, NY, United States

CHRISTOS FALOUTSOS, Carnegie Mellon University, Pittsburgh, PA, United States

Graph Evolution: Densification and Shrinking Diameters

JURE LESKOVEC
Carnegie Mellon University
JON KLEINBERG
Cornell University
and
CHRISTOS FALOUTSOS
Carnegie Mellon University

How do real graphs evolve over time? What are normal growth patterns in social, technological, and information networks? Many studies have discovered patterns in *static graphs*, identifying properties in a single snapshot of a large network or in a very small number of snapshots; these include heavy tails for in- and out-degree distributions, communities, small-world phenomena, and others. However, given the lack of information about network evolution over long periods, it has been hard to convert these findings into statements about trends over time.

Here we study a wide range of real graphs, and we observe some surprising phenomena. First, most of these graphs densify over time with the number of edges growing superlinearly in the number of nodes. Second, the average distance between nodes often shrinks over time in contrast to the conventional wisdom that such distance parameters should increase slowly as a function of the number of nodes (like $O(\log n)$ or $O(\log(\log n))$.

Existing graph generation models do not exhibit these types of behavior even at a qualitative level. We provide a new graph generator, based on a forest fire spreading process that has a simple, intuitive justification, requires very few parameters (like the flammability of nodes), and produces graphs exhibiting the full range of properties observed both in prior work and in the present study.

This material is based on work supported by the National Science Foundation under Grants No. IIS-0209107 SENSOR-0329549 EF-0331657IIS-0326322 IIS- 0534205, CCF-0325453, IIS-0329064, CNS-0403340, CCR-0122581; a David and Lucile Packard Foundation Fellowship; and also by the Pennsylvania Infrastructure Technology Alliance (PITA), a partnership of Carnegie Mellon, Lehigh University and the Commonwealth of Pennsylvania's Department of Community and Economic Development (DCED). Additional funding was provided by a generous gift from Hewlett-Packard. J. Leskovec was partially supported by the Microsoft Research Graduate Fellowship. Any opinions, findings, and conclusions or recommendations expressed in this material are those of the author(s) and do not necessarily reflect the views of the National Science Foundation, or other funding parties.
Author's address: J. Leskovec, Machine Learning Department, School of Computer Science, Carnegie Mellon University, 5000 Forbes Avenue, 15213 Pittsburgh PA, USA; email: jure@cs.cmu.edu.

We also notice that the forest fire model exhibits a sharp transition between sparse graphs and graphs that are densifying. Graphs with decreasing distance between the nodes are generated around this transition point.

Last, we analyze the connection between the temporal evolution of the degree distribution and densification of a graph. We find that the two are fundamentally related. We also observe that real networks exhibit this type of relation between densification and the degree distribution.

Categories and Subject Descriptors: H.2.8 [**Database Management**]: Database Applications—*Data mining*

General Terms: Measurement, Theory

Additional Key Words and Phrases: Densification power laws, graph generators, graph mining, heavy-tailed distributions, small-world phenomena

ACM Reference Format:

Leskovec, J., Kleinberg, J., and Faloutsos, C. 2007. Graph evolution: Densification and shrinking diameters. ACM Trans. Knowl. Discov. Data 1, 1, Article 2 (March 2007), 41 pages. DOI = 10.1145/1217299.1217301 http://doi.acm.org/10.1145/1217299.1217301

1. INTRODUCTION

In recent years, there has been considerable interest in graph structures in technological, sociological, and scientific settings: computer networks (routers or autonomous systems connected together); networks of users exchanging email or instant messages; citation networks and hyperlink networks; social networks (who trusts whom, who talks to whom, etc.); and countless more [Newman 2003]. The study of such networks has proceeded along two related tracks: the measurement of large network datasets, and the development of random graph models that approximate the observed properties.

Many of the properties of interest in these studies are based on two fundamental parameters, namely, the nodes' *degrees* (i.e., the number of edges incident to each node), and the *distances* between pairs of nodes (as measured by shortest-path length). The node-to-node distances are often studied in terms of the *diameter*—the maximum distance—and a set of closely related but more robust quantities including the average distance among pairs and the *effective diameter* (the 90th percentile distance, a smoothed form of which we use for our studies).

Almost all large real-world networks evolve over time by the addition and deletion of nodes and edges. Most of the recent models of network evolution capture the growth process in a way that incorporates two pieces of conventional wisdom:

(1) *Constant average degree assumption.* The average node degree in the network remains constant over time. (Or equivalently, the number of edges grows linearly in the number of nodes.)
(2) *Slowly growing diameter assumption.* The diameter is a slowly growing function of the network size, as in small world graphs [Albert et al. 1999; Broder et al. 2000b; Milgram 1967; Watts et al. 1998].

For example, the intensively-studied *preferential attachment model* [Albert and Barabasi 1999; Newman 2003] posits a network in which each new node,

when it arrives, attaches to the existing network by a constant number of outlinks, according to a rich-get-richer rule. Recent work has given tight asymptotic bounds on the diameter of preferential attachment networks [Bollobas and Riordan 2004; Chung and Lu 2002]; depending on the precise model, these bounds grow logarithmically [Krapivsky and Redner 2005] or even slower than logarithmically in the number of nodes.

How are assumptions (1) and (2) reflected in data on network growth? Empirical studies of large networks to date have mainly focused on *static* graphs, identifying properties of a single snapshot or a very small number of snapshots of a large network. For example, despite the intense interest in the Web's link structure, the recent work of Ntoulas et al. [2004] noted the lack of prior empirical research on the evolution of the Web. Thus, while one can assert based on these studies that real networks qualitatively have relatively small average node degrees and diameters, it has not been clear how to convert these into statements about trends over time.

1.1 The Present Work: Densification Laws and Shrinking Diameters

Here we study a range of different networks from several domains, and we focus specifically on the way in which fundamental network properties vary with time. We find, based on the growth patterns of these networks, that principles (1) and (2) need to be reassessed. Specifically, we show the following for a broad range of networks across diverse domains.

(1′) *Empirical observation: densification power laws.* The networks are becoming denser over time with the average degree increasing (and hence with the number of edges growing superlinearly in the number of nodes). Moreover, the densification follows a power-law pattern.

(2′) *Empirical observation: shrinking diameters.* The effective diameter is, in many cases, actually decreasing as the network grows.

We view the second of these findings as particularly surprising: Rather than shedding light on the long-running debate over exactly how slowly the graph diameter grows as a function of the number of nodes, it suggests a need to revisit standard models so as to produce graphs in which the effective diameter is capable of actually shrinking over time. We also note that, while densification and decreasing diameters are properties that are intuitively consistent with one another (and are both born out in the datasets we study), they are qualitatively distinct in the sense that it is possible to construct examples of graphs evolving over time that exhibit one of these properties but not the other.

We can further sharpen the quantitative aspects of these findings. In particular, the densification of these graphs, as suggested by (1′), is not arbitrary; we find that as the graphs evolve over time, they follow a version of the relation

$$e(t) \propto n(t)^a, \tag{1}$$

where $e(t)$ and $n(t)$ denote the number of edges and nodes of the graph at time t, and a is an exponent that generally lies strictly between 1 and 2. We refer to such a relation as a *densification power law*, or *growth power law*. (Exponent $a = 1$

corresponds to constant average degree over time, while $a = 2$ corresponds to an extremely dense graph where each node has, on average, edges to a constant fraction of all nodes.)

What underlying process causes a graph to systematically densify with a fixed exponent as in Equation (1) and to experience a decrease in effective diameter even as its size increases? This question motivates the second main contribution of this work. We present two families of probabilistic generative models for graphs that capture aspects of these properties. The first model, which we refer to as *Community Guided Attachment* (CGA) [Leskovec et al. 2005], argues that graph densification can have a simple underlying basis; it is based on a decomposition of the nodes into a nested set of communities such that the difficulty of forming links between communities increases with the community size. For this model, we obtain rigorous results showing that a natural tunable parameter in the model can lead to a densification power law with any desired exponent a. The second model, which is more sophisticated, exhibits both densification and a decreasing effective diameter as it grows. This model, which we refer to as the *Forest Fire Model*, is based on having new nodes attach to the network by burning through existing edges in epidemic fashion. The mathematical analysis of this model appears to lead to novel questions about random graphs that are quite complex, but, through simulation, we find that, for a range of parameter values, the model exhibits realistic behavior in densification, distances, and degree distributions. It is thus the first model to our knowledge that exhibits this full set of desired properties.

Accurate properties of network growth, together with models supporting them, have implications in several contexts.

—*Graph generation.* Our findings form means for assessing the quality of graph generators. Synthetic graphs are important for what if scenarios, for extrapolations, and for simulations when real graphs are impossible to collect (e.g., a very large friendship graph between people).
—*Graph sampling.* Datasets consisting of huge real-world graphs are increasingly available with sizes ranging from the millions to billions of nodes. There are many known algorithms to compute interesting measures (shortest paths, centrality, betweenness, etc.), but most of these algorithms become impractical for large graphs. Thus sampling is essential, but sampling from a graph is a nontrivial problem since the goal is to maintain structural properties of the network. Densification laws can help discard bad sampling methods, by providing means to reject sampled subgraphs.

A recent work of Leskovec and Faloutsos [2006] proposed two views on sampling from large graphs. For *back-in-time* sampling, the goal is to find a sequence of sampled subgraphs that matches the evolution of the original graph and thus obey the temporal growth patterns. On the other hand, *scale-down* sampling aims for a sample that matches the properties of the original large graph. The authors considered various sampling strategies, propose evaluation techniques, and use the temporal graph patterns presented in this article to evaluate the quality of the sampled subgraphs.

—*Extrapolations.* For several real graphs, we have a lot of snapshots of their past. What can we say about their future? Our results help form a basis for validating scenarios for graph evolution.

—*Abnormality detection and computer network management.* In many network settings, normal behavior will produce subgraphs that obey densification laws (with a predictable exponent) and other properties of network growth. If we detect activity-producing structures that deviate significantly from this, we can flag it as an abnormality. This can potentially help with the detection of, for instance, fraud, spam, or distributed denial-of-service (DDoS) attacks.

The rest of the article is organized as follows: Section 2 surveys the related work. Section 3 gives our empirical findings on real-world networks across diverse domains. Section 4 describes our proposed models and gives results obtained both through analysis and simulation. Section 5 gives the formal and experimental analysis of the relationship between the degree distribution and the graph densification over time. We conclude and discuss the implications of our findings in Section 6.

2. RELATED WORK

Research over the past few years has identified classes of properties that many real-world networks obey. One of the main areas of focus has been on *degree power laws*, which show that the set of node degrees has a heavy-tailed distribution. Such degree distributions have been identified in phones call graphs [Abello et al. 1998], the Internet [Faloutsos et al. 1999], the Web [Albert and Barabasi 1999; Huberman and Adamic 1999; Kumar et al. 1999], click-stream data [Bi et al. 2001], and for a who-trusts-whom social network [Chakrabarti et al. 2004]. Other properties include the small-world phenomenon, popularly known as six-degrees-of-separation, which states that real graphs have surprisingly small (average or effective) diameter (see Albert et al. [1999]; Bollobas and Riordan [2004]; Broder et al. [2000b]; Chung and Lu [2002]; Kleinberg [2002]; Milgram [1967]; Watts et al. [1998; 2002]).

In parallel with empirical studies of large networks, there has been considerable work on probabilistic models for graph generation. The discovery of degree power laws led to the development of random graph models that exhibited such degree distributions, including the family of models based on preferential attachment [Albert and Barabasi 1999; Abello et al. 2002; Cooper and Frieze 2003], copying model [Kleinberg et al. 1999; Kumar et al. 2000], and the related growing network with redirection model [Krapivsky and Redner 2001], which produces graphs with constant diameter and logarithmically increasing average degree [Krapivsky and Redner 2005].

Similar to our Forest Fire Model is the work of Vazquez [2001; 2003] wherein ideas based on random walks and recursive search for generating networks were introduced. In a random walk model, the walk starts at a random node, follows links, and, for each visited node, with some probability an edge is created between the visited node and the new node. It can be shown that such a model will generate graphs with power-law degree distribution with exponent $\gamma \geq 2$. On the other hand, in the recursive search model, first a new

node is added to the network, and the edge to a random node is created. If an edge is created to a node in the network, then, with some probability q, an edge is also created to each of its 1-hop neighbors. This rule is recursively applied until no edges are created. The recursive search model is similar to our Forest Fire Model in the sense that it exploits current network structure to create new edges. However, there is an important difference; in the recursive search model, the average degree scales at most logarithmically (and not as a power law) with the number of nodes in the network. Our simulation experiments also indicated that the diameter of networks generated by the recursive search does not decrease over time, but either slowly increases or remains constant.

We point the reader to Mitzenmacher [2004], Newman [2003], and Alderson et al. [2005] for overviews of this area. Recent work of Chakrabarti and Faloutsos [2006] gives a survey of the properties of real-world graphs and the underlying generative models for graphs.

It is important to note the fundamental contrast between one of our main findings here—that the average number of out-links per Node is growing polynomially in the network size—and the body of work on degree-power laws. This earlier work developed models that almost exclusively used the assumption of node degrees that were bounded by constants (or at most logarithmic functions) as the network grew; our findings and associated model challenge this assumption by showing that networks across a number of domains become denser over time.

Dorogovtsev and Mendes in a series of works [2001a, 2001b, 2003] analyzed possible scenarios of nonlinearly growing networks while maintaining scale-free structure. Among considered hypothetical scenarios were also those where the number of links grows polynomially with the number of edges, that is densification power law, while maintaining power-law degree distribution. The authors call this an *accelerated growth* and propose preferential attachment-type models where densification is forced by introducing an additional node attractiveness factor that is not only degree-dependent but also time-dependent. The motivation for their work comes from the fact that authors Broder et al. [2000a] and Faloutsos et al. [1999] reported the increase of the average degree over time on the Web and the Internet. Our work here differs in that it presents measurements on many time-evolving networks to support our findings and proposes generative models where densification is an emerging property of the model. Besides densification, we also address the shrinking diameters and consider models for generating them.

The bulk of prior work on the empirical study of network datasets has focused on static graphs, identifying patterns in a single snapshot or a small number of network snapshots (see also the discussion of this point by Ntoulas et al. [2004]). Two exceptions are the very recent work of Katz [2005], who independently discovered densification power laws for citation networks, and the work of Redner [2004], who studied the evolution of the citation graph of *Physical Review* over the past century. Katz's work builds on his earlier research on power-law relationships between the size and the recognition of professional communities [Katz 1999]; his work on densification is focused specifically on

citations, and he does not propose a generative network model to account for the densification phenomenon as we do here. Redner's work focuses on a range of citation patterns over time which are different from the network properties we study.

Our Community Guided Attachment (CGA) model, which produces densifying graphs, is an example of a hierarchical graph generation model in which the linkage probability between nodes decreases as a function of their relative distance in the hierarchy [Chakrabarti et al. 2004; Kleinberg 2002; Watts et al. 2002; Leskovec et al. 2005; Leskovec et al. 2005; Abello 2004]. Again, there is a distinction between the aims of this past work and our model. While these earlier network models were seeking to capture properties of individual snapshots of a graph, we seek to explain a time evolution process in which one of the fundamental parameters, the average node degree, is varying as the process unfolds. Our Forest Fire Model follows the overall framework of earlier graph models in which nodes arrive one at a time and link into the existing structure. Like the copying model discussed earlier, for example, a new node creates links by consulting the links of existing nodes. However, the recursive process by which nodes in the Forest Fire Model creates these links is quite different, leading to the new properties discussed in the previous section.

This article extends the work of Leskovec et al. [2005] by introducing new measurements and analysis of the evolution of degree distribution and its connection to densification power law. In a follow-up paper [Leskovec et al. 2005], we introduced *Kronecker Graphs*, a mathematically tractable model of graph growth and evolution. Kronecker graphs are based on tensor products of graph adjacency matrices and exhibit a full set of static and temporal graph properties. The emphasis of the work on Kronecker graphs is focused the ability to prove theorems about their properties and not to provide simple generative models like our Forest Fire model that intrinsically lead to densification and shrinking diameter.

3. OBSERVATIONS

We study the temporal evolution of several networks by observing snapshots of these networks taken at regularly spaced points in time. We use datasets from seven different sources. For each, we have information about the time when each node was added to the network over a period of several years which enables the construction of a snapshot at any desired point in time. For each of the datasets, we find a version of the densification power law from Equation (1), $e(t) \propto n(t)^a$; the exponent a differs across datasets, but remains remarkably stable over time. We also find that the effective diameter decreases in all the datasets considered.

The datasets consist of two citation graphs for different areas in the physics literature, a citation graph for U.S. patents, a graph of the Internet, five bipartite affiliation graphs of authors with papers they authored, a recommendation network, and an email communication network. Overall then, we consider 12 different datasets from 7 different sources.

3.1 Densification Laws

We now describe the datasets we used, and our findings related to densification. For each graph dataset, we have, or can generate, several time snapshots for which we study the number of nodes $n(t)$ and the number of edges $e(t)$ at each timestamp t. We denote by n and e the final number of nodes and edges. We use the term *Densification Power Law plot* (or just DPL plot) to refer to the log-log plot of number of edges $e(t)$ versus number of nodes $n(t)$.

3.1.1 *ArXiv Citation Graph.* We first investigate a citation graph provided as part of the 2003 KDD Cup [Gehrke et al. 2003]. The HEP–TH (high energy physics theory) citation graph from the e-print arXiv covers all the citations within a dataset of $n = 29{,}555$ papers with $e = 352{,}807$ edges. If a paper i cites paper j, the graph contains a directed edge from i to j. If a paper cites, or is cited by, a paper outside the dataset, the graph does not contain any information about this. We refer to this dataset as *arXiv*.

This data covers papers in the period from January 1993 to April 2003 (124 months). It begins within a few months of the inception of the arXiv, and thus represents essentially the complete history of its HEP–TH section. For each month m ($1 \leq m \leq 124$), we create a citation graph using all papers published up to month m. For each of these graphs, we plot the number of nodes versus the number of edges on a logarithmic scale and fit a line.

Figure 2(a) shows the DPL plot; the slope is $a = 1.68$ and corresponds to the exponent in the densification law. Notice that a is significantly higher than 1, indicating a large deviation from linear growth. As noted earlier, when a graph has $a > 1$, its average degree increases over time. Figure 1(a) plots exactly the average degree $\bar{d}$ over time, and it is clear that $\bar{d}$ increases. This means that the average length of the bibliographies of papers increases over time.

There is a subtle point here that we elaborate upon next. With almost any network dataset, one does not have data reaching all the way back to the network's birth (to the extent that this is a well-defined notion). We refer to this as the problem of the *missing past*. Due to this, there will be some effect of increasing out-degree simply because edges will point to nodes prior to the beginning of the observation period, that is, over time fewer references are pointing to papers outside the dataset. We refer to such nodes as *phantom nodes*, with a similar definition for *phantom edges*. In all our datasets, we find that this effect is relatively minor once we move away from the beginning of the observation period; the phenomenon of increasing degree continues through to the present. For example, in arXiv, nodes over the most recent years are primarily referencing nonphantom nodes; we observe a knee in Figure 1(a) in 1997 that appears to be attributable in large part to the effect of phantom nodes. (Later, when we consider a graph of the Internet, we will see a case where comparable properties hold in the absence of any missing past issues.) A similar observation of growing reference lists over time was also independently made by Krapivsky and Redner [2005].

We also experimented with a second citation graph, taken from the HEP–PH section of the arXiv, which is about the same size as our first arXiv dataset. It exhibits the same behavior, with the densification exponent $a = 1.56$. The plot

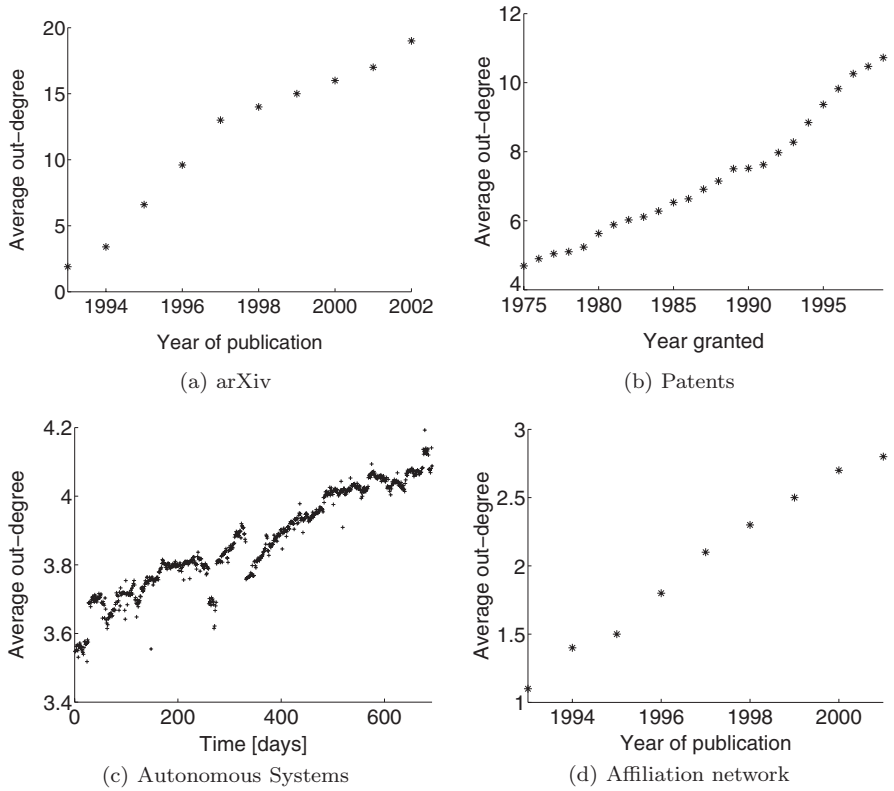

(a) arXiv (b) Patents

(c) Autonomous Systems (d) Affiliation network

Fig. 1. The average node out-degree over time. Notice that it increases, in all 4 datasets, that is, all graphs are densifying.

is omitted for brevity but we show the summary of results on all 11 datasets we considered in Table I.

3.1.2 *Patents Citation Graph.* Next, we consider a U.S. patent dataset maintained by the National Bureau of Economic Research [Hall et al. 2001]. The data set spans 37 years (January 1, 1963 to December 30, 1999) and includes all the utility patents granted during that period, totaling $n = 3{,}923{,}922$ patents. The citation graph includes all citations made by patents granted between 1975 and 1999, totaling $e = 16{,}522{,}438$ citations. For the patents dataset, there are 1,803,511 nodes for which we have no information about their citations (we only have the in-links). Because the dataset begins in 1975, it too has a missing past issue, but again the effect of this is minor as one moves away from the first few years.

The patents data also contains citations outside the dataset. For patents outside the dataset, the time is unknown. These patents have zero out-degree and are at some time cited by the patents from within the dataset. We set the time (grant year) of these out-of-dataset patents to the year when they were first cited by a patent from the dataset. This is natural and is equivalent to saying that patents for which the grant year is unknown are in the dataset

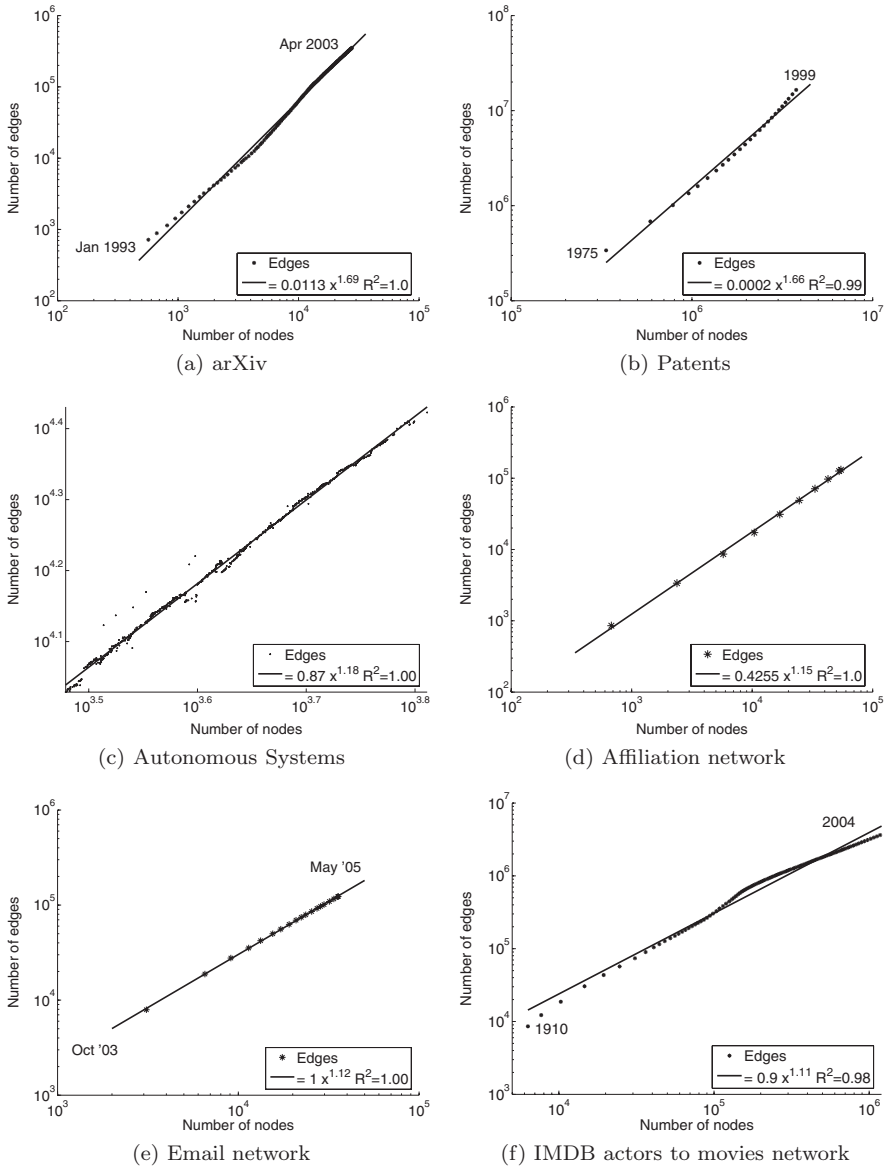

(a) arXiv (b) Patents

(c) Autonomous Systems (d) Affiliation network

(e) Email network (f) IMDB actors to movies network

Fig. 2. Number of edges $e(t)$ versus number of nodes $n(t)$ in log-log scales for several graphs. All 4 graphs obey the densification power law with a consistently good fit. Slopes: $a = 1.68$, 1.66, 1.18, 1.15, 1.12, and 1.11, respectively.

from the beginning but when counting, we count only nonzero degree nodes. So the time when we first count an unknown patent is when it gets a first link.

We follow the same procedure as with arXiv. For each year Y from 1975 to 1999, we create a citation network on patents up to year Y and give the DPL plotin Figure 2(b). As with the arXiv citation network, we observe a high densification exponent, in this case $a = 1.66$.

Table I. Dataset Names with Sizes, Time Lengths and Densification Power Law Exponents
Notice the very high densification exponent for citation networks (≈ 1.6), around 1.2 for Autonomous Systems, and lower (but still significant) densification exponent (≈ 1.1) for affiliation and collaboration type networks

Dataset	Nodes	Edges	Time	DPL exponent
Arxiv HEP–PH	30,501	347,268	124 months	1.56
Arxiv HEP–TH	29,555	352,807	124 months	1.68
Patents	3,923,922	16,522,438	37 years	1.66
AS	6,474	26,467	785 days	1.18
Affiliation ASTRO–PH	57,381	133,179	10 years	1.15
Affiliation COND–MAT	62,085	108,182	10 years	1.10
Affiliation GR-QC	19,309	26,169	10 years	1.08
Affiliation HEP–PH	51,037	89,163	10 years	1.08
Affiliation HEP–TH	45,280	68,695	10 years	1.08
Email	35,756	123,254	18 months	1.12
IMDB	1,230,276	3,790,667	114 years	1.11
Recommendations	3,943,084	15,656,121	710 days	1.26

Figure 1(b) illustrates the increasing out-degree of patents over time. Note that this plot does not incur any of the complications of a bounded observation period since the patents in the dataset include complete citation lists, and we are simply plotting the average size of these as a function of the year.

3.1.3 *Autonomous Systems Graph.* The graph of routers comprising the Internet can be organized into subgraphs called Autonomous Systems (AS). Each AS exchanges traffic flows with some neighbors (peers). We can construct a communication network of who-talks-to-whom from the BGP (Border Gateway Protocol) logs.

We use the Autonomous Systems (AS) dataset from Oregon [1997]. The dataset contains 735 daily instances which span an interval of 785 days from November 8 1997 to January 2 2000. The graphs range in size from $n = 3{,}011$ nodes and $e = 10{,}687$ edges to the largest AS graph that has $n = 6{,}474$ nodes and $e = 26{,}467$ edges.

In contrast to citation networks where nodes and edges only get added (not deleted) over time, the AS dataset also exhibits both the addition and deletion of the nodes and edges over time.

Figure 2(c) shows the DPL plot for the Autonomous Systems dataset. We observe a clear trend: even in the presence of noise, changing external conditions, and disruptions to the Internet we observe a strong superlinear growth in the number of edges over more than 700 AS graphs. We show the increase in the average node degree over time in Figure 1(c). The densification exponent is $a = 1.18$, lower than the one for the citation networks, but still clearly greater than 1.

3.1.4 *Affiliation Graphs.* Using the arXiv data, we also constructed bipartite *affiliation graphs*. There is a node for each paper, a node for each person who authored at least one arXiv paper, and an edge connecting people to the papers they authored. Note that the more traditional *coauthorship network* is implicit in the affiliation network: two people are coauthors if there is at least one paper joined by an edge to each of them.

We studied affiliation networks derived from the five largest categories in the arXiv (ASTRO–PH, HEP–TH, HEP–PH, COND–MAT and GR–QC). We place a timestamp on each node: the submission date of each paper and, for each person, the date of their first submission to the arXiv. The data for affiliation graphs covers the period from April 1992 to March 2002. The smallest of the graphs (category GR–QC) had 19,309 nodes (5,855 authors, 13,454 papers) and 26,169 edges. ASTRO–PH is the largest graph, with 57,381 nodes (19,393 authors, 37,988 papers) and 133,170 edges. It has 6.87 authors per paper; most of the other categories also have similarly high numbers of authors per paper.

For all these affiliation graphs, we observe similar phenomena, and, in particular, we have densification exponents between 1.08 and 1.15. We present the complete set of measurements only for ASTRO–PH, the largest affiliation graph. Figures 1(d) and 2(d) show the increasing average degree over time, and a densification exponent of $a = 1.15$. Table I shows the sizes and densification power law exponents for other four affiliation graphs.

3.1.5 *Email Network.* We also considered an email network from a large European research institution. For a period from October 2003 to May 2005 (18 months), we have anonymized information about all incoming and outgoing email of the research institution. For each sent or received email message, we know the time, the sender, and the recipient of the email. Overall we have 3,038,531 emails covering 287,755 different email addresses. Note that we have a complete email graph for only 1,258 email addresses that come from the research institution. Furthermore, there are 35,756 email addresses that both sent and received email within the span of our dataset. All other email addresses are either nonexisting, mistyped, or spam.

Given a set of email messages, we need to create a graph. Since there can be multiple emails sent between the same two addresses (nodes), we follow the practice of Kossinets and Watts [2006]. Given a set of email messages, each node corresponds to an email address. We create an edge between nodes i and j if they exchanged messages both ways, that is, i sent at least one message to j, and j sent at least one message to i.

Similar to citation networks, we take all email messages up to a particular time t and create a graph using the procedure previously described. So, in the first month, we observe 254,080 emails between 38,090 different addresses. Using the procedure [Kossinets and Watts 2006] of generating a graph from a set of emails, we get $n = 6{,}537$ nodes and $e = 18{,}812$ edges. After 18 months, at the end of the dataset, we have $n = 35{,}756$ nodes and $e = 123{,}254$ edges.

Figure 2(e) presents the DPL plot for the email network. Observe a clear trend: the email network is densifying regardless of the fact that it is growing and that new parts of the social network (email address space) are being explored. The densification exponent is $a = 1.12$, lower than the one for the citation networks but more similar to those from affiliation networks. Still clearly greater than 1.

Note that there is one issue with this dataset: we have complete information about all sent and received emails only for the core of the network (1,258 email addresses from the institution). For the rest of the addresses, the nodes on

the periphery, we only have their communication (links) with the core of the network.

Regardless of how we look at the email network, it always densifies. If we consider only the core of the network, the densification is very high. This is expected since the number of nodes (people at the research institution) basically remains constant over time, and the edges can only be added, not deleted, and densification naturally occurs.

The network also densifies if we consider the core plus the periphery, but when determining edges, we take a 2-month sliding window [Kossinets and Watts 2006]. This means that for every month m, we take all email messages between $m - 2$ and m, and create a graph where there is an edge if nodes exchanged emails both ways in the last 2 months. This graph also densifies with densification exponent $a = 1.21$.

Interestingly, the sliding window email network has a higher densification exponent than the full evolving email network. A possible explanation is that email usage is increasing over time and not all nodes (email addresses) are active at all times. Over the 18 month time period, the size of 2-month sliding window graphs increases from 7,000 to 10,000 nodes. On the other hand, the full email graph (composed of all nodes up to month m) grows from 3,000 to 38,000 nodes over the same time period. This means that there is a large number of email addresses that are active only for a period of time. In a moving window graph, we observe only active users and thus more edges since email usage has also increased and people communicate more. As opposed to the evolution of the full email network, the moving window graphs do not have to accumulate the history, that is, sparse graphs from the past, so they densify faster.

3.1.6 *IMDB Actors-to-Movies Network.* The Internet Movie Data Base (IMDB, `http://www.imdb.com`) is a collection of facts about movies and actors. For every movie we know the year of production, genre, and actor names that appeared in the movie. From IMDB, we obtained data about 896,192 actors and 334,084 movies produced between 1890 and 2004 (114 years).

Given this data, we created a bipartite graph of actors-to-movies the same way as in the case of affiliation networks. This means that, whenever a new movie appears, it links to all the actors participating in it. We create a new actor node when the actor first appears in any movie. This way, when a new movie appears, we first create a movie node, then we introduce actor nodes, but only for actors for whom this was their first appearance in a movie. Then we link actors and the movie.

In our experiment, we started observing the graph in 1910 when the giant connected component started to form. Before 1910, the largest connected component consisted of less than 15% of the nodes. At the beginning of our observation period, the network had $n = 7{,}690$ nodes (4,219 actors and 3,471 movies) and $e = 12{,}243$ edges. At the end of the dataset in 2004, we have $n = 1{,}230{,}276$ nodes and $e = 3{,}790{,}667$ edges.

We follow the usual procedure, that is, for every year Y, we take all the movies up to year Y and actors that appeared in them. We create a graph and measure how the number of edges grows with the number of nodes. Figure 2(f)

presents the DPL plot for the IMDB actors-to-movies network. Again, notice the nontrivial densification exponent of $a = 1.11$.

3.1.7 *Product Recommendation Network.* We also report the analysis of Leskovec et al. [2006], where they measured the densification of a large person-to-person recommendation network from a large online retailer. Nodes represent people and edges represent recommendations. The network generation process was as follows. Each time a person purchases a book, music CD, or a movie, he or she is given the option of sending emails recommending the item to friends. Any of the recipients of the recommendation that makes a purchase can further recommend the item, and through this propagation of recommendations, the network forms.

The network consists of $e = 15{,}646{,}121$ recommendations made among $n = 3{,}943{,}084$ distinct users. The data was collected from June 5 2001 to May 16 2003. In total, 548,523 products were recommended. We report the densification power law exponent $a = 1.26$ in Table I.

3.2 Shrinking Diameters

We now discuss the behavior of the effective diameter over time for this collection of network datasets. Following the conventional wisdom on this topic, we expected the underlying question to be whether we could detect the differences among competing hypotheses concerning the growth rates of the diameter, for example, the difference between logarithmic and sublogarithmic growth. Thus, it was with some surprise that we found the effective diameters to be actually decreasing over time (Figure 3).

Let us define the necessary concepts underlying the observations. We say that two nodes in a network are *connected* if there is an undirected path between them; for each natural number d, let $g(d)$ denote the fraction of connected node pairs whose shortest connecting path has length at most d. The *hop-plot* for the network is the set of pairs $(d, g(d))$; it thus gives the cumulative distribution of distances between connected node pairs. We extend the hop-plot to a function defined over all positive real numbers by linearly interpolating between the points $(d, g(d))$ and $(d+1, g(d+1))$ for each d, and we define the *effective diameter* of the network to be the value of d at which the function $g(d)$ achieves the value 0.9.

Definition 3.1. Graph G has the diameter d if the maximum length of undirected shortest path over all connected pairs of nodes is d. The length of the path is the number of segments (edges, links, hops) it contains.

We also use *full diameter* to refer to this quantity. Notice the difference between the usual definition of the diameter and ours. For a disconnected graph, the diameter is usually defined to be infinite, here we avoid this problem by considering only pairs of nodes that are connected. Also note that we ignore the directionality of an edge if the graph is directed.

Definition 3.2. For each natural number d, let $g(d)$ denote the fraction of connected node pairs whose undirected shortest connecting path in a graph G

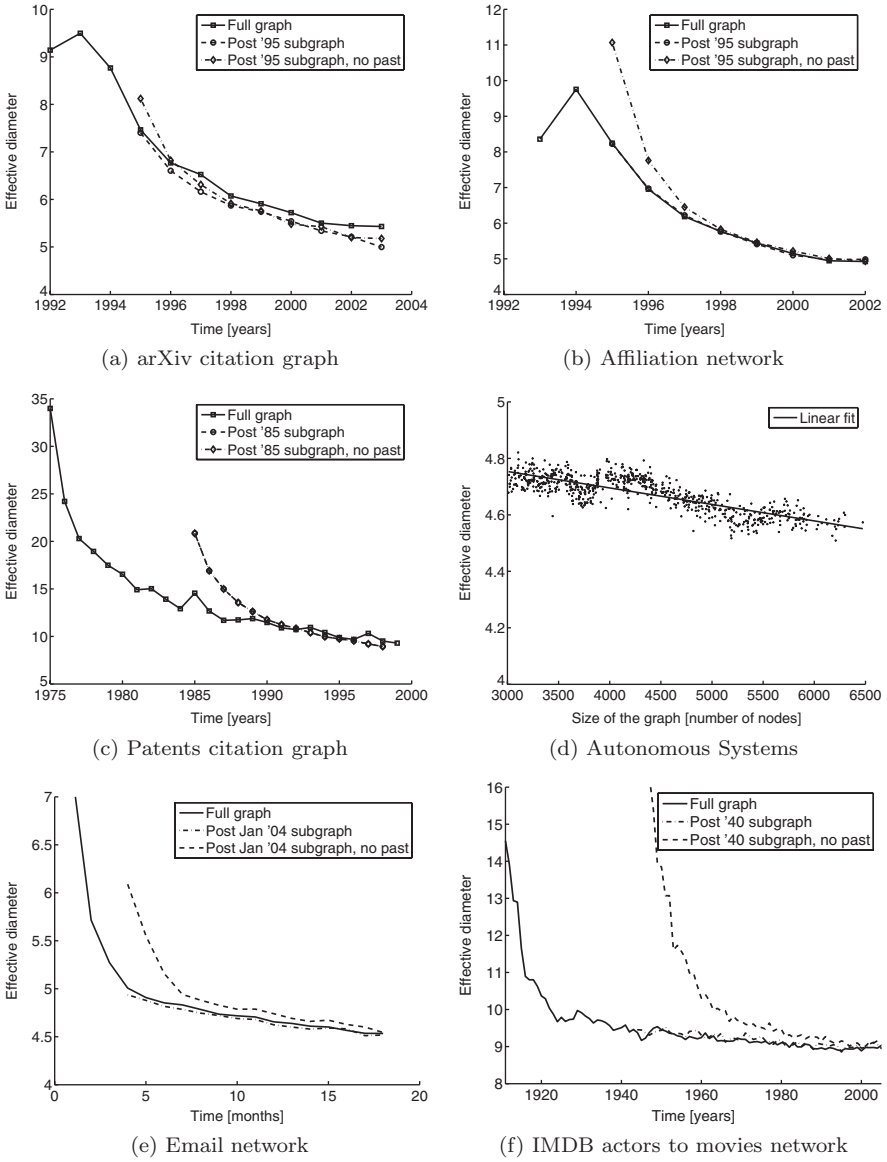

(a) arXiv citation graph (b) Affiliation network

(c) Patents citation graph (d) Autonomous Systems

(e) Email network (f) IMDB actors to movies network

Fig. 3. The effective diameter over time for 6 different datasets. Notice the consistent decrease of the diameter over time.

has length at most d. And let D be an integer for which $g(D-1) < 0.9$ and $g(D) \geq 0.9$. Then the graph G has the *integer effective diameter* D [Tauro et al. 2001].

In other words, the integer effective diameter is the smallest number of hops D at which at least 90% of all connected pairs of nodes can be reached.

Last we give the definition of the *effective diameter* as considered in this article. Originally we defined $g(d)$, a fraction of connected pairs of nodes at

distance at most d, only for natural numbers d. Now we extend the definition of g to all positive reals x by linearly interpolating the function value between $g(d)$ and $g(d+1)$ $(d \leq x < d+1)$: $g(x) = g(d) + (g(d+1) - g(d))(x - d)$.

Definition 3.3. Let D be a value where $g(D) = 0.9$. Then graph G has the effective diameter D.

This definition varies slightly from an alternate definition of the effective diameter used in earlier work: the minimum integer value d such that at least 90% of the connected node pairs are at distance at most d. Our variation smooths this definition by allowing it to take noninteger values.

The effective diameter is a more robust quantity than the diameter (defined as the maximum distance over all connected node pairs) since the diameter is prone to the effects of degenerate structures in the graph (e.g., very long chains). However, our experiments show that the effective diameter and diameter tend to exhibit qualitatively similar behavior. Note that under these definitions, the effective diameter and the diameter are well defined even if the graph is disconnected.

We follow the same procedure as in case of densification power law measurements. For each time t, we create a graph consisting of nodes up to that time and compute the effective diameter of the undirected version of the graph.

Figure 3 shows the effective diameter over time; one observes a decreasing trend for all the graphs. We performed a comparable analysis to what we describe here for all 11 graph datasets in our study with very similar results. For the citation networks in our study, the decreasing effective diameter has the following interpretation. Since all the links out of a node are frozen at the moment it joins the graph, the decreasing distance between pairs of nodes appears to be the result of subsequent papers acting as bridges by citing earlier papers from disparate areas. Note that for other graphs in our study, such as the AS dataset, it is possible for an edge between two nodes to appear at an arbitrary time after these two nodes join the graph.

We note that the effective diameter of a graph over time is necessarily bounded from below, and the decreasing patterns of the effective diameter in the plots of Figure 3 are consistent with convergence to some asymptotic value. However, understanding the full limiting behavior of the effective diameter over time to the extent that this is even a well-defined notion remains an open question.

3.2.1 *Validating the Shrinking Diameter Conclusion.* Given the unexpected nature of this result, we wanted to verify that the shrinking diameters were not attributable to artifacts of our datasets or analyses. We explored this issue in a number of ways, which we now summarize; the conclusion is that the shrinking diameter appears to be a robust, and intrinsic, phenomenon. Specifically, we performed experiments to account for (a) possible sampling problems, (b) the effect of disconnected components, (c) the effect of the missing past (as in the previous section), and (d) the dynamics of the emergence of the giant component.

—*Possible sampling problems.* Computing shortest paths among all node pairs is computationally prohibitive for graphs of our scale. We used several different approximate methods, obtaining almost identical results from all of them. In particular, we applied the Approximate Neighborhood Function (ANF) approach [Palmer et al. 2002] (in two different implementations), which can estimate effective diameters for very large graphs, as well as a basic sampling approach in which we ran exhaustive breadth-first search from a subset of the nodes chosen uniformly at random. The results using all these methods were essentially identical.

Plots on Figure 3 were created by averaging over 100 runs of the ANF, the approximate diameter algorithm. For all datasets, the standard error is less than 10%. For clarity of presentation, we do not show the error bars.

—*Disconnected components.* One can also ask about the effect of small disconnected components. All of our graphs have a single *giant component*—a connected component (or a weakly connected component in the case of directed graphs, ignoring the direction of the edges)—that accounts for a significant fraction of all nodes. For each graph, we computed effective diameters for both the entire graph and just the giant component; again, our results are essentially the same using these two methods.

—*Missing past effects.* A third issue is the problem of the missing past, the same general issue that surfaced in the previous section when we considered densification. In particular, we must decide how to handle citations to papers that predate our earliest recorded time. (Note that the missing past is not an issue for the AS network data where the effective diameter also decreases.)

To understand how the diameters of our networks are affected by this unavoidable problem, we perform the following test. We pick some positive time $t_0 > 0$ and determine what the diameter would look like as a function of time if this were the beginning of our data. We then put back in the nodes and the edges from before time t_0 and study how much the diameters change. If this change is small—or at least if it does not affect the qualitative conclusions—then it provides evidence that the missing past is not influencing the overall result.

Specifically, we set this cut-off time t_0 at the beginning of 1995 for the arXiv (since we have data from 1993), and at 1985 for the patent citation graph (we have data from 1975). For the email network, we set the cut-off time to January 2004 and for IMDB to 1940 (we also experimented with 1920 and 1960 and findings were consistent). We then compared the results of three measurements.

(i) *Diameter of full graph.* For each time t, we compute the effective diameter of the graph's giant component.

(ii) *Post-t_0 subgraph.* We compute the effective diameter of the post-t_0 subgraph using all nodes and edges. This means that, for each time t ($t > t_0$), we create a graph using all nodes dated before t. We then compute the effective diameter of the subgraph of the nodes dated between t_0 and t. To compute the effective diameter, we can use all edges and nodes (including

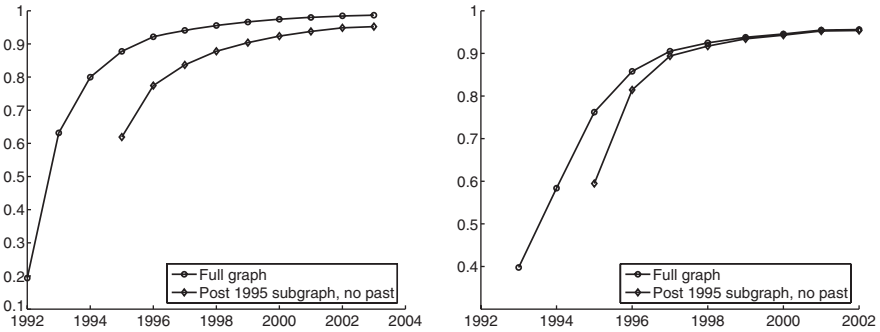

(a) arXiv citation graph (b) Affiliation network

Fig. 4. The fraction of nodes that are part of the giant connected component over time. We see that, after 4 years, the 90% of all nodes in the graph belong to the giant component.

those dated before t_0). This means that we are measuring distances only among nodes dated between t_0 and t while also using nodes and edges before t_0 as shortcuts or bypasses. The experiment measures the diameter of the graph if we knew the full (pre-t_0) past, the citations of the papers which we have intentionally excluded for this test.

(iii) *Post-t_0 subgraph, no past.* We set t_0 the same way as in the previous experiment, but then, for all nodes dated before t_0, we delete all their outlinks. This creates the graph we would have gotten if we had started collecting data only at time t_0.

In Figure 3, we superimpose the effective diameters using the three different techniques. If the missing past does not play a large role in the diameter, then all three curves should lie close to one another. We observe this is the case for the arXiv citation graphs. For the arXiv paper-author affiliation graph and for the patent citation graph, the curves are quite different right at the cut-off time t_0 (where the effect of deleted edges is most pronounced), but they quickly align with one another. As a result, it seems clear that the continued decreasing trend in the effective diameter as time runs to the present is not the result of these boundary effects.

—*Emergence of the giant component.* A final issue is the dynamics by which the giant component emerges. For example, in the standard Erdös-Renyi random graph model (which has a substantially different flavor from the growth dynamics of the graphs here), the diameter of the giant component is quite large when it first appears, and then it shrinks as edges continue to be added. Could shrinking diameters in some way be a symptom of the emergence of giant component?

It appears fairly clear that this is not the case. Figure 4 shows the fraction of all nodes that are part of the largest connected component (GCC) over time. We plot the size of the GCC for the full graph and for a graph where we had no past, that is, where we delete all outlinks of the nodes dated before the cut-off time t_0. Because we delete the outlinks of the pre-t_0 nodes, the size of the GCC

Table II. Table of Symbols

Symbol	Description
a	*Densification Exponent*
c	*Difficulty Constant*
$f(h)$	*Difficulty Function*
$n(t)$	number of nodes at time t
$e(t)$	number of edges at time t
b	community branching factor
$\bar{d}$	expected average node out-degree
H	height of the tree
$h(v, w)$	least common ancestor height of leaves v, w
p	forest fire forward burning probability
p_b	forest fire backward burning probability
r	ratio of backward and forward probability, $r = p/p_b$
γ	power-law degree distribution exponent

is smaller, but, as the graph grows, the effect of these deleted links becomes negligible.

We see that, within a few years, the giant component accounts for almost all the nodes in the graph. The effective diameter, however, continues to steadily decrease beyond this point. This indicates that the decrease is happening in a mature graph and not because many small disconnected components are being rapidly glued together.

Based on all this, we believe that the decreasing diameters in our study reflect a fundamental property of the underlying networks. Understanding the possible causes of this property as well as the causes of the densification power laws discussed earlier will be the subject of the next section.

4. PROPOSED MODELS

We have now seen that densification power laws and shrinking effective diameters are properties that hold across a range of diverse networks. Moreover, existing models do not capture these phenomena. We would like to find some simple, local model of behavior which could naturally lead to the macroscopic phenomena we have observed. We present increasingly sophisticated models, all of which naturally achieve the observed densification. The last one (the Forest Fire model) also exhibits shrinking diameter and all the other main patterns known (including heavy-tailed in- and out-degree distributions). Table II summarizes the symbols used in our discussion.

4.1 Community Guided Attachment

What are the underlying principles that drive all our observed graphs to obey a densification power law without central control or coordination? We seek a model in which the densification exponent arises from intrinsic features of the process that generates nodes and edges. While one could clearly define a graph model in which $e(t) \propto n(t)^a$ by simply having each node, when it arrives at time t, generate $n(t)^{a-1}$ outlinks, the equivalent of positing that each author of a paper in a citation network has a rule like "Cite n^{a-1} other documents," hardwired in his or her brain. Such a model would not provide any insight into

the origin of the exponent a as the exponent is unrelated to the operational details by which the network is being constructed. Instead, our goal is to see how underlying properties of the network evolution process itself can affect the observed densification behavior.

We take the following approach. Power laws often appear in combination with *self-similar* structures. Intuitively, a self-similar object consists of miniature replicas of itself [Schroeder 1991]. Our approach involves two steps both of which are based on self-similarity.

We begin by searching for self-similar recursive structures. In fact, we can easily find several such recursive sets, for example, computer networks form tight groups (e.g., based on geography), which consist of smaller groups, and so on, recursively. Similarly for patents: they also form conceptual groups (chemistry, communications, etc.), which consist of subgroups, and so on, recursively. Several other graphs feature such communities-within-communities patterns.

For example, it has been argued (see e.g. Watts et al. [2002] and the references therein) that social structures exhibit self-similarity with individuals organizing their social contacts hierarchically. Moreover, pairs of individuals belonging to the same small community form social ties more easily than pairs of individuals who are only related by membership in a larger community. In a different domain, Menczer studied the frequency of links among Web pages that are organized into a topic hierarchy such as the Open Directory [Menczer 2002]. He showed that link density among pages decreases with the height of their least common ancestor in the hierarchy. That is, two pages on closely related topics are more likely to be hyperlinked than are two pages on more distantly related topics.

This is the first, qualitative step in our explanation for the densification power law. The second step is quantitative. We will need a numerical measure of the difficulty in crossing communities. The extent to which it is indeed difficult to form links across communities will be a property of the domain being studied. We call this the *difficulty constant*, and we define it more precisely in the following.

4.1.1 *The Basic Version of the Model.* We represent the recursive structure of communities-within-communities as a tree Γ of height H. We shall show that even a simple perfectly-balanced tree of constant fanout b is enough to lead to a densification power law, and so we will focus the analysis on this basic model.

The nodes V in the graph we construct will be the leaves of the tree, that is, $n = |V|$. (Note that $n = b^H$.) Let $h(v, w)$ define the standard tree distance of two leaf nodes v and w, that is, $h(v, w)$ is the height of their least common ancestor (the height of the smallest subtree containing both v and w).

We will construct a random graph on a set of nodes V by specifying the probability that v and w form an edge as a function f of $h(v, w)$. We refer to this function f as the *difficulty function*. What should form of f be the? Clearly, it should decrease with h, but there are many forms such a decrease could take.

The form of f that works best for our purposes comes from the self-similarity arguments we made earlier: We would like f to be scale-free, that is, $f(h)/f(h-1)$ should be level-independent and thus constant. The only way to achieve level

independence is to define $f(h) = f(0)c^{-h}$. Setting $f(0)$ to 1 for simplicity, we have:

$$f(h) = c^{-h}, \tag{2}$$

where $c \geq 1$. We refer to the constant c as the difficulty constant. Intuitively, cross-communities links become harder to form as c increases.

This completes our development of the model which we refer to as *Community Guided Attachment*: If the nodes of a graph belong to communities-within-communities, and if the cost for cross-community edges is scale-free (Equation (2)), the densification power law follows naturally. No central control or exogenous regulations are needed to force the resulting graph to obey this property. In short, self-similarity itself leads to the densification power law.

THEOREM 4.1. *In the Community Guided Attachment random graph model just defined, the expected average out-degree $\bar{d}$ of a node is proportional to:*

$$\begin{aligned} \bar{d} &= n^{1-\log_b(c)} && \text{if } 1 \leq c \leq b \\ &= \log_b(n) && \text{if } c = b \\ &= constant && \text{if } c > b \end{aligned}$$

PROOF. For a given node v, the expected out-degree (number of links) $\bar{d}$ of the node is proportional to

$$\bar{d} = \sum_{x \neq v} f(h(x,v)) = \sum_{j=1}^{\log_b(n)} (b-1)b^{j-1}c^{-j} = \frac{b-1}{c} \sum_{j=1}^{\log_b(n)} \left(\frac{b}{c}\right)^{j-1}. \tag{3}$$

There are three different cases. if $1 \leq c < b$, then by summing the geometric series, we obtain

$$\begin{aligned} \bar{d} &= \frac{b-1}{c} \cdot \frac{\left(\frac{b}{c}\right)^{\log_b(n)} - 1}{\left(\frac{b}{c}\right) - 1} = \left(\frac{b-1}{b-c}\right)(n^{1-\log_b(c)} - 1) \\ &= \Theta(n^{1-\log_b(c)}). \end{aligned}$$

In the case when $c = b$, the series sums to

$$\begin{aligned} \bar{d} &= \sum_{x \neq v} f(h(x,v)) = \frac{b-1}{b} \sum_{j=1}^{\log_b(n)} \left(\frac{b}{b}\right)^{j-1} = \frac{b-1}{b} \log_b(n) \\ &= \Theta(\log_b(n)). \end{aligned}$$

The last case is when the difficulty constant c is greater than the branching factor b ($c > b$); then the sum in Equation (3) converges to a constant even if carried out to infinity, and so we obtain $\bar{d} = \Theta(1)$. □

Note that when $c < b$, we get a densification law with exponent greater than 1: the expected out-degree is $n^{1-\log_b(c)}$, and so the total number of edges grows as n^a, where $a = 2 - \log_b(c)$. Moreover, as c varies over the interval $[1, b)$, the exponent a ranges over all values in the interval $(1, 2]$.

COROLLARY 4.2. *If the difficulty function is scale-free ($f(h) = c^{-h}$, with $1 < c < b$), then the Community Guided Attachment obeys the densification power law with exponent*

$$a = 2 - \log_b(c).$$

4.1.2 *Dynamic Community Guided Attachment.* So far, we have discussed a model in which nodes are first organized into a nested set of communities, and then they start forming links. We now extend this to a setting in which nodes are added over time, and the nested structure deepens to accommodate them. We will assume that a node only creates outlinks at the moment it is added (and hence, only to nodes already present); this is natural for domains like citation networks in which a paper's citations are written at the same time as the paper itself.

Specifically, the model is as follows. Rather than having graph nodes reside only at the leaves of the tree Γ, there will now be a graph node corresponding to every internal node of Γ as well. Initially, there is a single node v in the graph, and our tree Γ consists just of v. In time step t, we go from a complete b-ary tree of depth $t-1$ to one of depth t, by adding b new leaves as children of each current leaf. Each of these new leaves will contain a new node of the graph.

Now, each new node forms outlinks according to a variant of the process in which all graph nodes are leaves. However, since a new node has the ability to link to internal nodes of the existing tree not just to other leaves, we need to extend the model to incorporate this. Thus, we define the *tree-distance* $d(v, w)$ between nodes v and w to be the length of a path between them in Γ—this is the length of the path from v up to the least common ancestor of v and w, plus the length of the path from this least common ancestor down to w. Note that if v and w are both leaves, then $d(v, w) = 2h(v, w)$, following our definition of $h(v, w)$.

The process of forming outlinks is as follows. For a constant c, node v forms a link to each node w, independently, with probability $c^{-d(v,w)/2}$. (Note that dividing by 2 in the exponent means this model gives the same probability as the basic model in the case when both v and w are leaves.)

Like the first model, this process produces a densification law with exponent $a = 2 - \log_b(c)$ when $c < b$. However, for $c < b^2$, it also yields a heavy-tailed distribution of in-degrees, something that the basic model did not produce. We describe this in the following theorem.

THEOREM 4.3. *The Dynamic Community Guided Attachment model just defined has the following properties.*

—*When $c < b$, the average node degree is $n^{1-\log_b(c)}$ and the in-degrees follow a Zipf distribution with exponent $\frac{1}{2}\log_b(c)$.*

—*When $b < c < b^2$, the average node degree is constant, and the in-degrees follow a Zipf distribution with exponent $1 - \frac{1}{2}\log_b(c)$.*

—*When $c > b^2$, the average node degree is constant and the probability of an in-degree exceeding any constant bound k decreases exponentially in k.*

PROOF. In the proof, all logarithms will be expressed in base b unless specified otherwise.

We begin with the following basic facts. If a node is at height h in the tree, then the number of nodes at distance $d \leq h$ from it is $\Theta(b^d)$. Nodes at distance $d > h$ can be reached by going up for j steps, and then down for $d - j$ steps (if $d - j \leq h + j$). This is maximized for $j = (d - h)/2$, and so the total number of nodes reachable at distance d is $\Theta(b^{(d+h)/2})$.

Case 1: $c < b$. In this case, the expected out-degree for a leaf node is

$$\sum_{d=0}^{2\log n} \Theta\left(\frac{b^{d/2}}{c^{d/2}}\right) = \Theta\left(\frac{b^{\log n}}{c^{\log n}}\right) = \Theta\left(\frac{n}{c^{\log n}}\right) = \Theta(n^{1-\log c}).$$

Since the expected out-degree values for other nodes are smaller, and since a constant fraction of all nodes are leaves, it follows that the expected value of the out-degree taken over all nodes is $\Theta(n^{1-\log c})$ as well.

Now we compute the expected in-degree of a node at height h. This is

$$\sum_{d \leq h} \Theta\left(\frac{b^d}{c^{d/2}}\right) + \sum_{d > h} \Theta\left(\frac{b^{(d+h)/2}}{c^{d/2}}\right) = \sum_{d \leq h} \Theta\left(\frac{b^{d/2}}{c^{d/2}}\right) b^{d/2} + \sum_{d > h} \Theta\left(\frac{b^{d/2}}{c^{d/2}}\right) b^{h/2}.$$

The largest term in this sum is the last, for $d = 2\log n - h$. Here it takes the value

$$\Theta\left(\frac{b^{\log n}}{c^{\log n - (h/2)}}\right) = \Theta\left(\frac{b^{\log n}}{c^{\log n}}\right) c^{h/2} = \Theta(n^{1-\log c} c^{h/2}).$$

The maximum expected in-degree z is achieved for $h = \log n$, when we get

$$z = \Theta(n^{1-\log c} c^{.5\log n}) = \Theta(n^{1-.5\log c}).$$

So for a node at depth $t = \log n - h$, we get an expected in-degree of

$$\Theta(n^{1-\log c} c^{(\log n - t)/2}) = \Theta(z c^{-t/2}).$$

Hence, to compute a Zipf exponent, we see that a node of degree rank $r = b^t$ has depth t, so it has degree

$$\Theta\left(\frac{z}{c^{t/2}}\right) = \Theta\left(\frac{z}{r^{.5\log c}}\right).$$

Case 2: $b < c < b^2$. In this case, the expected out-degree for a leaf node is

$$\sum_{d=0}^{2\log n} \Theta\left(\frac{b^{d/2}}{c^{d/2}}\right) = \Theta(1).$$

Since the expected out-degree values for other nodes are smaller, it follows that the expected value of the out-degree taken over all nodes is $\Theta(1)$ as well.

Now we compute the expected in-degree of a node at height h. This is

$$\sum_{d \leq h} \Theta\left(\frac{b^d}{c^{d/2}}\right) + \sum_{d > h} \Theta\left(\frac{b^{(d+h)/2}}{c^{d/2}}\right) = \sum_{d \leq h} \Theta\left(\frac{b^{d/2}}{c^{d/2}}\right) b^{d/2} + \sum_{d > h} \Theta\left(\frac{b^{d/2}}{c^{d/2}}\right) b^{h/2}.$$

Since $b < c < b^2$, these terms increase geometrically up to $d = h$, then decrease. Thus, the largest term is for $d = h$, where it is $\Theta(b^h c^{-h/2})$.

Thus the maximum degree is $z = \Theta(n^{1-.5\log c})$, and for depth $t = \log n - h$, we get a degree of

$$\Theta\left(\left(\frac{b}{c^{1/2}}\right)^{\log n}\left(\frac{b}{c^{1/2}}\right)^{-t}\right) = \Theta\left(z\left(\frac{b}{c^{1/2}}\right)^{-t}\right).$$

Now, $b/c^{1/2} = b^{1-.5\log c}$, so a node of degree rank $r = b^t$ (at depth t) has degree $\Theta(z/r^{1-.5\log c})$.

Case 3: $c > b^2$. The expected out-degrees here are only smaller than they are in the previous case, and hence the expected value of the out-degree taken over all nodes is $\Theta(1)$.

The node whose in-degree is most likely to exceed a fixed bound k is the root, at height $h = \log n$. The in-degree of the root is a sum X of independent 0-1 random variables X_v, where X_v takes the value 1 if node v links to the root, and X_v takes the value 0 otherwise. We have

$$EX = \sum_v EX_v = \sum_{d \le \log n} \Theta\left(\frac{b^d}{c^{d/2}}\right) = \Theta(1),$$

and hence by Chernoff bounds, the probability that it exceeds a given value $k > EX$ decreases exponentially in k. □

Thus, the dynamic Community Guided Attachment model exhibits three qualitatively different behaviors as the parameter c varies: densification with heavy-tailed in-degrees, then constant average degree with heavy-tailed in-degrees, and then constant in- and out-degrees with high probability. Note also the interesting fact that the Zipf exponent is maximized for the value of c right at the onset of densification.

Finally, we have experimented with versions of the dynamic Community Guided Attachment model in which the tree is not balanced, but rather deepens more on the left branches than the right (in a recursive fashion). We have also considered versions in which a single graph node can reside at two different nodes of the tree Γ, allowing for graph nodes to be members of different communities. Experimental results and overall conclusions were always the same and consistent regardless of the particular version (modification) of the dynamic Community Guided Attachment model used.

4.2 The Forest Fire Model

Community Guided Attachment and its extensions show how densification can arise naturally and even in conjunction with heavy-tailed in-degree distributions. However, it is not a rich enough class of models to capture all the properties in our network datasets. In particular, we would like to capture both the shrinking effective diameters that we have observed as well as the fact that real networks tend to have heavy-tailed out-degree distributions (though generally not as skewed as their in-degree distributions). The Community Guided Attachment models do not exhibit either of these properties.

Specifically, our goal is as follows. Given a (possibly empty) initial graph G, and a sequence of new nodes $v_1 \ldots v_k$, we want to design a simple randomized process to successively link v_i to nodes of G $(i = 1, \ldots k)$ so that the resulting graph G_{final} will obey all of the following patterns: heavy-tailed distributions for in- and out-degrees, the densification power law, and shrinking effective diameter.

We are guided by the intuition that such a graph generator may arise from a combination of the following components:

—some type of rich-get-richer attachment process to lead to heavy-tailed in-degrees;
—some flavor of the copying model [Kumar et al. 2000] to lead to communities;
—some flavor of Community Guided Attachment to produce a version of the densification power law; and
—a yet unknown ingredient to lead to shrinking diameters.

Note that we will not be assuming a community hierarchy on nodes, and so it is not enough to simply vary the Community Guided Attachment model.

Based on this, we introduce the Forest Fire Model, which is capable of producing all these properties. To set up this model, we begin with some intuition that also underpinned Community Guided Attachment: nodes arrive in over time; each node has a center-of-gravity in some part of the network; and its probability of linking to other nodes decreases rapidly with their distance from this center-of-gravity. However, we add to this picture the notion that, occasionally a new node will produce a very large number of outlinks. Such nodes will help cause a more skewed out-degree distribution; they will also serve as bridges that connect formerly disparate parts of the network, bringing the diameter down.

4.2.1 *The Basic Forest Fire Model.* Following this plan, we now define the most basic version of the model. Essentially, nodes arrive one at a time and form outlinks to some subset of the earlier nodes; to form outlinks, a new node v attaches to a node w in the existing graph, and then begins burning links outward from w, linking with a certain probability to any new node it discovers. One can view such a process as intuitively corresponding to a model by which an author of a paper identifies references to include in the bibliography. He or she finds a first paper to cite, chases a subset of the references in this paper (modeled here as random), and continues recursively with the papers discovered in this way. Depending on the bibliographic aids being used in this process, it may also be possible to chase backlinks to papers that cite the paper under consideration. Similar scenarios can be considered for social networks: a new computer science (CS) graduate student arrives at a university, meets some older CS students, who introduce him/her to their friends (CS or non-CS), and the introductions may continue recursively.

We formalize this process as follows, obtaining the Forest Fire Model. To begin with, we will need two parameters, a *forward burning probability* p, and a *backward burning ratio* r, whose roles will be described in the following.

Consider a node v joining the network at time $t > 1$, and let G_t be the graph constructed thus far. (G_1 will consist of just a single node.) Node v forms outlinks to nodes in G_t according to the following process.

(i) v first chooses an ambassador node w uniformly at random and forms a link to w.

(ii) We generate two random numbers, x and y, that are geometrically distributed with means $p/(1-p)$ and $rp/(1-rp)$, respectively. Node v selects x outlinks and y in-links of w incident to nodes that were not yet visited. Let $w_1, w_2, \ldots, w_{x+y}$ denotes the other ends of these selected links. If not enough in- or outlinks are available, v selects as many as it can.

(iii) v forms outlinks to $w_1, w_2, \ldots, w_{x+y}$, and then applies step (ii) recursively to each of $w_1, w_2, \ldots, w_{x+y}$. As the process continues, nodes cannot be visited a second time, preventing the construction from cycling.

Thus, the burning of links in the Forest Fire model begins at w, spreads to $w_1, \ldots, w_{x+y}$, and proceeds recursively until it dies out. In terms of the intuition from citations in papers, the author of a new paper v initially consults w, follows a subset of its references (potentially both forward and backward) to the papers $w_1, \ldots, w_{x+y}$, and then continues accumulating references recursively by consulting these papers. The key property of this model is that certain nodes produce large conflagrations, burning many edges and hence forming many outlinks before the process ends.

Despite the fact that there is no explicit hierarchy in the Forest Fire Model as there was in Community Guided Attachment, there are some subtle similarities between the models. Where a node in Community Guided Attachment was the child of a parent in the hierarchy, a node v in the Forest Fire Model also has an entry point via its chosen ambassador node w. Moreover, just as the probability of linking to a node in Community Guided Attachment decreased exponentially in the tree distance, the probability that a new node v burns k successive links so as to reach a node u lying k steps away is exponentially small in k. (Of course, in the Forest Fire Model, there may be many paths that could be burned from v to u, adding some complexity to this analogy.)

In fact, our Forest Fire Model combines the flavors of several older models and produces graphs qualitatively matching their properties. We establish this by simulation, as we now describe, but it is also useful to provide some intuition for why these properties arise.

—*Heavy-tailed in-degrees.* Our model has a rich-get-richer flavor: highly-linked nodes can easily be reached by a newcomer no matter which ambassador it starts from.

—*Communities.* The model also has a copying flavor: a newcomer copies several of the neighbors of his/her ambassador (and then continues this recursively).

—*Heavy-tailed out-degrees.* The recursive nature of link formation provides a reasonable chance for a new node to burn many edges and thus produce a large out-degree.

—*Densification power law.* A newcomer will have a lot of links near the community of his/her ambassador, a few links beyond this, and significantly fewer farther away. Intuitively, this is analogous to the Community Guided Attachment, although without an explicit set of communities.

—*Shrinking diameter.* It is not a priori clear why the Forest Fire Model should exhibit a shrinking diameter as it grows. Graph densification is helpful in reducing the diameter, but it is important to note that densification is certainly not enough on its own to imply shrinking diameter. For example, the Community Guided Attachment model obeys the densification power law, but our experiments also show that the diameter slowly increases (not shown here for brevity).

Rigorous analysis of the Forest Fire Model appears to be quite difficult. However, in simulations, we find that by varying just the two parameters p and r, we can produce graphs that densify ($a > 1$), exhibit heavy-tailed distributions for both in- and out-degrees (Figure 6), and have diameters that decrease. This is illustrated in Figure 5, which shows plots for the effective diameter and the densification power law exponent as a function of the number of nodes for some selections of p and r.

We see that, depending on the forward and backward burning parameters, the Forest Fire Model is capable of generating sparse or dense graphs with effective diameters that either increase or decrease, while also producing power-law in- and out-degree distributions (Figure 6). Informally, a dense graph has close to a linear number of edges incident to each node, while a sparse graph has significantly fewer than a linear number of edges incident to each node.

Also notice the high sensitivity of the parameter space. We fix the forward-burning probability p, and by increasing the backward-burning probability p_b for only a few percent, we move from an increasing to a slowly and then to a more rapidly decreasing effective diameter (Figure 5).

Figure 7 plots the evolution of the effective diameter of Forest Fire. We generated a single large graph on 250,000 nodes and measured the effective diameter over time. Error bars present 1 standard deviation of the estimated effective diameter over 10 runs. Both plots show the same data. The left figure plots the number of nodes on linear while the right plots the log number of nodes. Notice the convergence of the effective diameter. At first it shrinks more rapidly, and then slowly converges to a low value.

4.2.2 *Extensions to the Forest Fire Model.* Our basic version of the Forest Fire Model exhibits rich structure with just two parameters. By extending the model in natural ways, we can fit observed network data even more closely. We propose two natural extensions: orphans and multiple ambassadors.

Orphans. In both the patent and arXiv citation graphs, there are many isolated nodes, that is, documents with no citations into the corpus. For example, many papers in the arXiv only cite non-arXiv papers. We refer to them as *orphans*. Our basic model does not produce orphans since each node always links at least to its chosen ambassador. However, it is easy to incorporate orphans into the model in two different ways. We can start our graphs with $n_0 > 1$ nodes

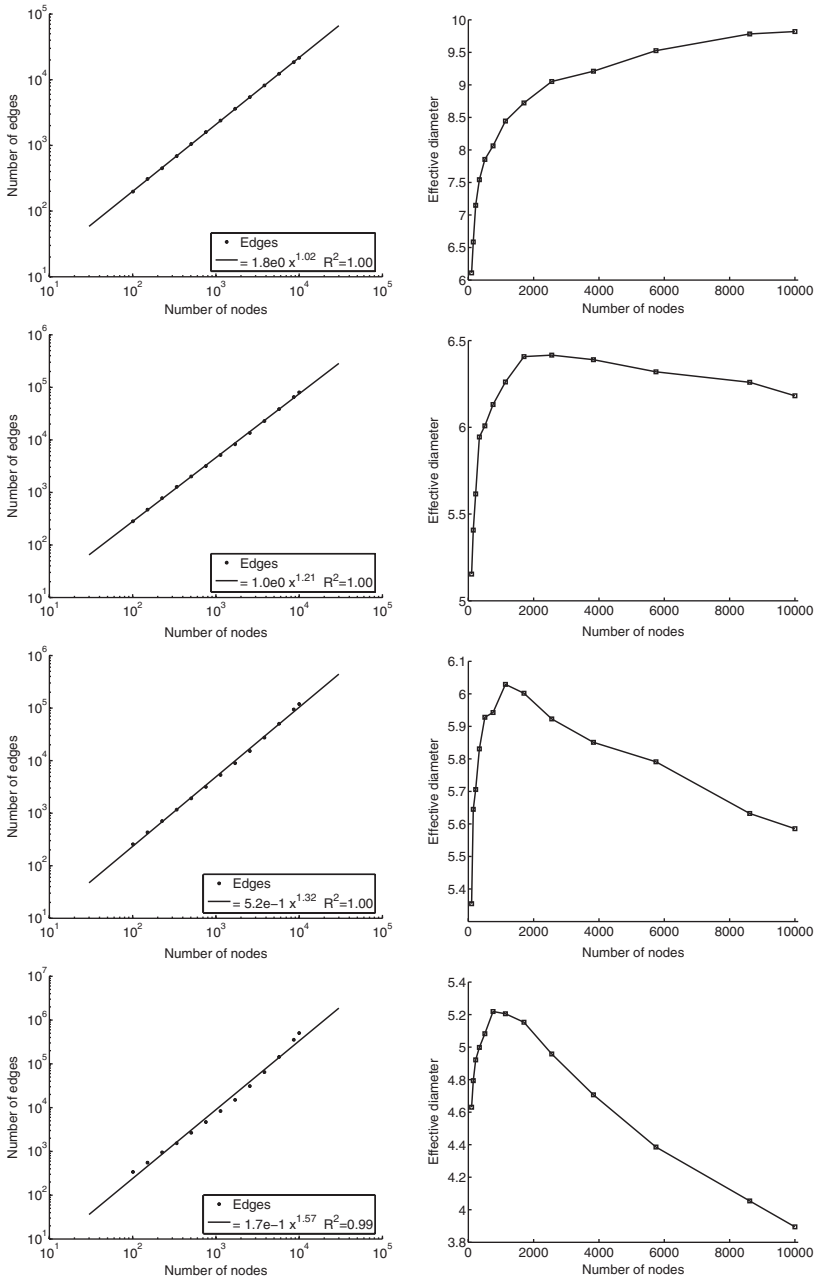

Fig. 5. The DPL plot and the diameter for the Forest Fire model. Row 1: sparse graph ($a = 1.01 < 2$), with increasing diameter (forward-burning probability: $p = 0.35$, backward probability: $p_b = 0.20$). Row 2: (most realistic case:) densifying graph ($a = 1.21 < 2$) with slowly decreasing diameter ($p = 0.37$, $p_b = 0.32$). Row 3: densifying graph (($a = 1.32 < 2$) with decreasing diameter ($p = 0.37$, $p_b = 0.33$). Row 4: dense graph with densification exponent close to 2 ($a = 1.57$) and decreasing diameter ($p = 0.38$, $p_b = 0.35$).

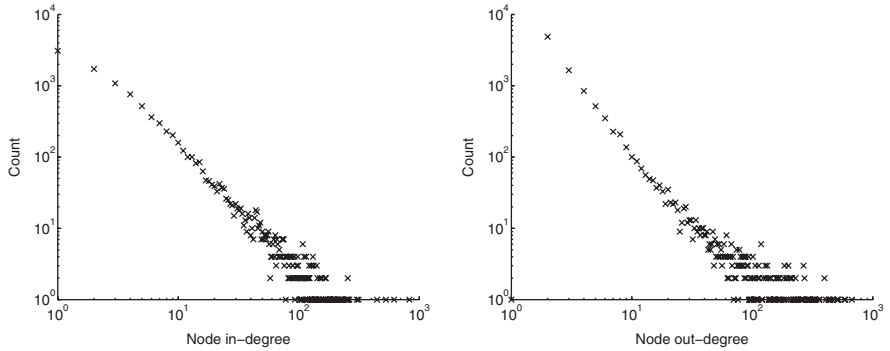

In-degree Out-degree

Fig. 6. Degree distribution of a sparse graph with decreasing diameter (forward-burning probability: 0.37, backward probability: 0.32).

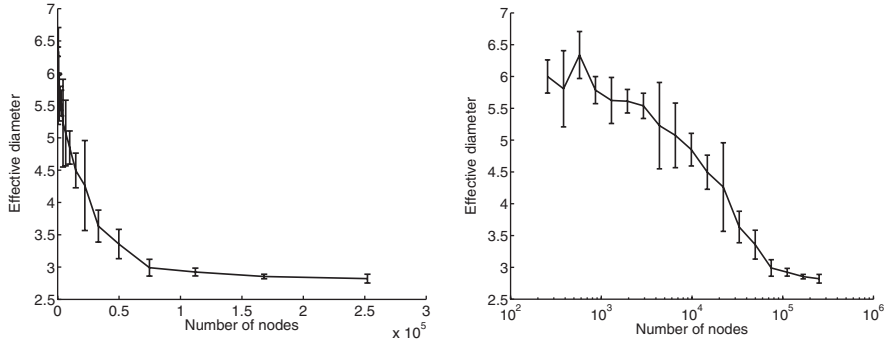

(a) Effective diameter $p = 0.37$, $p_b = 0.34$

(b) Effective diameter (log nodes) $p = 0.37$, $p_b = 0.34$

Fig. 7. Evolution of effective diameter of the Forest Fire model while generating a large graph. Both plots show the same data; the left one plots on linear scales and the right one plots on log-linear scales (effective diameter vs. log number of nodes). Error bars show the confidence interval of the estimated effective diameter. Notice that the effective diameter shrinks and then slowly converges.

at time $t = 1$, or we can have some probability $q > 0$ that a newcomer will form no links (not even to its ambassador) and so become an orphan.

We find that such variants of the model have a more pronounced decrease in the effective diameter over time, with large distances caused by groups of nodes linking to different orphans gradually diminishing as further nodes arrive to connect them together.

Multiple ambassadors. We experimented with allowing newcomers to choose more than one ambassador with some positive probability, that is, rather than burning links starting from just one node, there is some probability that a newly arriving node burns links starting from two or more. This extension also accentuates the decrease in effective diameter over time as nodes linking to multiple ambassadors serve to bring together formerly far-apart parts of the graph.

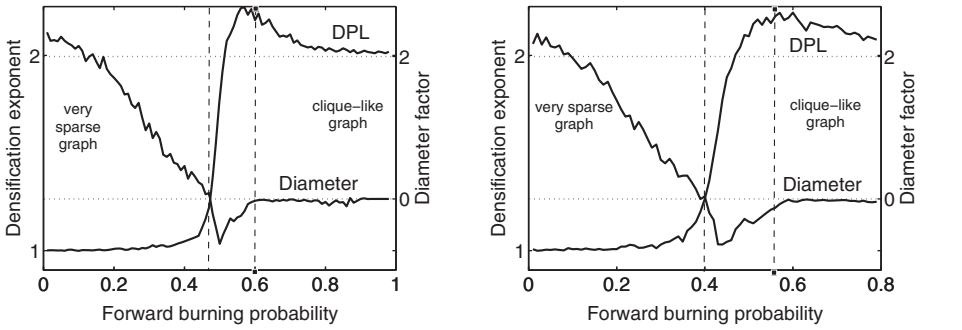

(a)We fix burning ratio, $r = 0.5$ and vary forward-burning probability p

(b) We fix backward-burning probability $p_b = 0.3$ and vary forward-burning probability p

Fig. 8. We vary the forward-burning probability while fixing burning ratio (a) or backward-burning probability (a). The plot gives a very precise cut through Forest Fire parameter space. Notice that each plot has two vertical axes: DPL exponent on the left, and the diameter log-fit factor on the right. Observe a very sharp transition in DPL exponent and a narrow region, indicated by vertical dashed lines, where Forest Fire produces slowly densifying graphs with decreasing effective diameter.

Burning a fixed percentage of neighbors. We also considered a version of Forest Fire where the fire burns a fixed percentage of node's edges, that is, the number of burned edges is proportional to the node's degree. When a fire comes into a node, for each unburned neighbor we independently flip a biased coin, and the fire spreads to nodes where the coin came up heads. This process continues recursively until no nodes are burned. In case of forward- and backward-burning probabilities, we have two coins, one for out- and one for in-edges.

The problem with this version of the model is that, once there is a single large fire that burns a large fraction of the graph, many subsequent fires will also burn much of the graph. This results in a bell-shaped, nonheavy-tailed degree distribution and gives two regimes of densification—slower densification before the first big fire, and quadratic ($a = 2$) densification afterwards.

We also experimented with the model where burning probability decayed exponentially as the fire moves away from the ambassador node.

4.2.3 *Phase Plot.* In order to understand the densification and the diameter properties of graphs produced by the Forest Fire Model, we explored the full parameter space of the basic model in terms of the two underlying parameters, the forward-burning probability p and the backward-burning ratio r.

Note there are two equivalent ways to parameterize the Forest Fire model. We can use the forward-burning probability p and the backward-burning ratio r or the forward-burning probability p and the backward-burning probability p_b ($p_b = rp$). We examine both and show two cuts through the parameter space.

Figure 8 shows how the densification exponent and the effective diameter depend on forward-burning probability p. In the left plot of Figure 8, we fix the backward-burning probability $p_b = 0.3$, and, in the right plot, we fix the backward-burning ratio $r = 0.5$. We vary forward-burning probability and plot the densification power law exponent. The densification exponent a is computed as in Section 3 by fitting a relation of the form $e(t) \propto n(t)^a$. Notice the very sharp

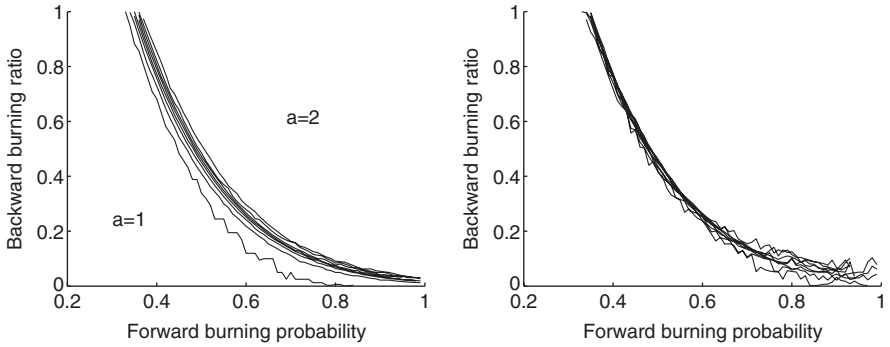

(a) Densification exponent (b) Diameter log-fit factor

Fig. 9. Contour plots: The densification power law exponent a (left) and the effective diameter log-fit factor α (right) over the parameter space (forward-burning probability and backward-burning ratio) of the Forest Fire model.

transition between the regimes with no densification and those with very high densification.

On the same plot we also show the effective diameter log-fit factor α. We fit a logarithmic function of the form diameter $= \alpha \log t + \beta$ (where t is the current time, and hence the current number of vertices) to the last half of the effective diameter plot; we then report the factor α. Thus, diameter factor $\alpha < 0$ corresponds to decreasing effective diameter over time, and $\alpha > 0$ corresponds to increasing effective diameter.

Going back to Figure 8, notice that at low values of forward-burning probability p, we observe increasing effective diameter and no densification ($a = 1$). As p increases, the effective diameter grows slower and slower. For a narrow band of p, we observe decreasing effective diameter, negative α (the small valley around $p = 0.45$). With high values of p, the effective diameter is constant ($\alpha \approx 0$), which means that the generated graph is effectively a clique with effective diameter close to 1 and DPL exponent $a \approx 2$. Also notice that the sharp transition in the DPL exponent and the decreasing effective diameter are very well aligned.

These simulations indicate that even the basic Forest Fire Model is able to produce sparse and slowly densifying (with densification exponent near 1) graphs in which the effective diameter decreases.

Figure 9 shows how the densification exponent and the effective diameter depend on the values of the Forest Fire parameters p and r.

Figure 9(a) gives the contour plot of the densification exponent a. The lower-left part corresponds to $a = 1$ (the graph maintains constant average degree), and, in the upper right part, $a = 2$—the graph is dense, that is, the number of edges grows quadratically with the number of nodes as, for example, in the case of a clique. The contours in between correspond to a 0.1 increase in DPL exponent: the left-most contour corresponds to $a = 1.1$ and the right-most contour corresponds to $a = 1.9$. The desirable region is in between; we observe that it is very narrow: a increases dramatically along a contour line, suggesting a sharp transition.

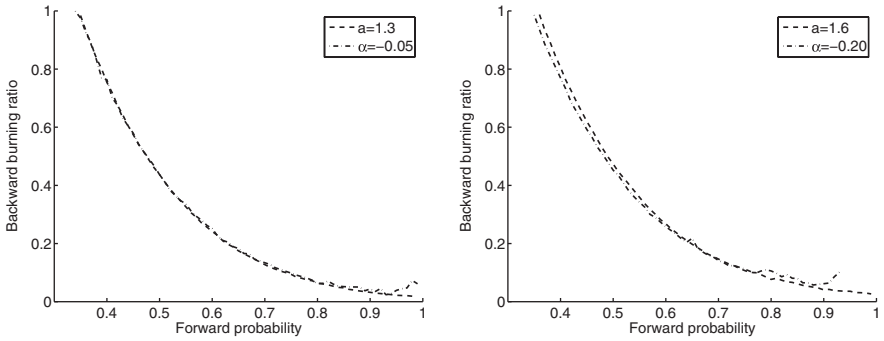

(a) Densification exponent $a = 1.3$
Diameter factor $\alpha = -0.05$

(b) Densification exponent $a = 1.6$
Diameter factor $\alpha = -0.20$

Fig. 10. We superimpose the densification power law exponent a and diameter log-fit α factor over the Forest Fire Model parameter space. Notice that the shape of the transition boundary of the densification and the shrinking diameter very much follow the same shape.

Figure 9(b) gives the contour plot for the effective diameter log-fit factor α as previously defined. Each contour corresponds to diameter factor α. We vary α in range $-0.3 \leq \alpha \leq 0.1$, with step-size 0.05. Notice, that the boundary in parameter space between decreasing and increasing effective diameter is very narrow.

Do contour plots of densification power law and shrinking diameters from Figure 9 follow the same shape? More exactly, does the boundary between decreasing and increasing diameters follow the same shape as the transition in the densification exponent?

We answer this question in Figure 10, where we superimpose phase contours of DPL and the effective diameter over the Forest Fire parameter space. The left plot superimposes phase contours for the densification power law exponent $a = 1.3$ and the diameter log-fit factor $\alpha = -0.05$. The right plot superimposes contours for $a = 1.6$ and $\alpha = -0.30$. In both cases we observe very good alignment of the two phase lines which suggests the same shape of the transition boundary for the densification power law exponent and the effective diameter.

We also observe similar behavior with orphans and multiple ambassadors. These additional features in the model help further separate the diameter decrease/increase boundary from the densification transition and so widen the region of parameter space for which the model produces reasonably sparse graphs with decreasing effective diameters.

5. DENSIFICATION AND THE DEGREE DISTRIBUTION OVER TIME

Many real-world graphs exhibit power-law degree distributions [Albert and Barabasi 1999; Faloutsos et al. 1999]. As we saw in Section 3, the average degree increases over time, and the graphs densify following the power-law relationship between the number of nodes and the number of edges. Here we analyze the relation between the densification and the power-law degree distribution over time and find evidence that some of the real world graphs obey

the relations we find. A similar analysis was also performed by Dorogovtsev and Mendes [2002], although without specific measurements or comparison to empirical data.

We analyze the following two cases. If the degree distribution of a time evolving graph is power-law, and it maintains constant power-law exponent γ over time, then we show that for $1 < \gamma < 2$, densification power law with exponent

$$a = 2/\gamma.$$

arises. In this case, the densification power law is the consequence of the fact that a power-law distribution with exponent $\gamma < 2$ has no finite expectation [Newman 2005], and thus the average degree grows as the degree exponent is constant.

Our second result is for the case when a temporally evolving graph densifies with densification exponent a and follows a power-law degree distribution with exponent $\gamma > 2$ that we alow to change over time. We show that, in this case, for a given densification exponent a, the power-law degree exponent γ_n has to evolve with the size of the graph n as

$$\gamma_n = \frac{4n^{a-1} - 1}{2n^{a-1} - 1}.$$

This shows that the densification power law and the degree distribution are related and that one implies the other.

5.1 Constant Degree Exponent Over Time

First, we analyze the case where the graph over time maintains power-law degree distribution with a constant exponent γ. Power law distribution $p(x) = cx^{-\gamma}$ with exponent $\gamma < 2$ has infinite expectation [Newman 2005], that is, as the number of samples increases, the mean also increases. Assuming that the exponent (slope) of the degree distribution does not change over time, a natural question to ask is: what is the relation between the densification power law exponent and the degree distribution over time? The following theorem answers the question.

THEOREM 5.1. *In a temporally evolving graph with a power-law degree distribution having constant degree exponent γ over time, the densification power law exponent a is:*

$$a = 1 \qquad \text{if } \gamma > 2 \tag{4}$$

$$= 2/\gamma \qquad \text{if } 1 \leq \gamma \leq 2 \tag{5}$$

$$= 2 \qquad \text{if } \gamma < 1 \tag{6}$$

PROOF. Assume that at any time t the degree distribution of an undirected graph G follows a power law. This means the number of nodes D_d with degree d is $D_d = cd^{-\gamma}$, where c is a constant. Now assume that at some point in time the maximum degree in the graph is d_{max}. Later, as the graph grows, we will let $d_{max} \to \infty$. Using the previous power-law relation, we can calculate the

number of nodes n and the number of edges e in the graph:

$$n = \sum_{d=1}^{d_{max}} cd^{-\gamma} \approx \int_{d=1}^{d_{max}} d^{-\gamma} = c\frac{d_{max}^{1-\gamma} - 1}{1-\gamma}$$
$$e = \frac{1}{2}\sum_{d=1}^{d_{max}} cd^{1-\gamma} \approx \int_{d=1}^{d_{max}} d^{1-\gamma} = c\frac{d_{max}^{2-\gamma} - 1}{2-\gamma}$$

Now, we let the graph grow, so $d_{max} \to \infty$. Then the densification power law exponent a is:

$$a = \lim_{d_{max}\to\infty} \frac{\log(e)}{\log(n)} = \frac{\gamma\log(d_{max}) + \log(|d_{max}^{2-\gamma} - 1|) - \log(|2-\gamma|)}{\gamma\log(d_{max}) + \log(|d_{max}^{1-\gamma} - 1|) - \log(|1-\gamma|)}.$$

Note, that the degree distribution exponent is γ, so we also have the relation $\log(c) = \gamma\log(d_{max})$. Now, we have 3, cases:

Case 1. $\gamma > 2$. No densification.

$$a = \frac{\gamma\log(d_{max}) + o(1)}{\gamma\log(d_{max}) + o(1)} = 1.$$

Case 2. $1 < \gamma < 2$ is the interesting case where densification arises.

$$a = \frac{\gamma\log(d_{max}) + (2-\gamma)\log(d_{max}) + o(1)}{\gamma\log(d_{max}) + o(1)} = \frac{2}{\gamma}.$$

Case 3. $1 < \gamma$. Maximum densification. The graph is basically a clique and the number of edges grows quadratically with the number of nodes.

$$a = \frac{\gamma\log(d_{max}) + (2-\gamma)\log(d_{max}) + o(1)}{\gamma\log(d_{max}) + (1-\gamma)\log(d_{max}) + o(1)} = 2.$$

□

This shows that for cases when a graph evolves by maintaining the constant power-law degree exponent $\gamma > 2$ over time, it does not densify. However, for cases when $ddslope < 2$, we observe densification. This can easily be explained. The densification means that the number of edges grows faster than the number of nodes. So, for densification to appear, the tail of the degree distribution has to grow, that is, it has to accumulate more mass over time. Here, this is the case since power-law distributions with exponent $\gamma < 2$ have no finite expectation. In the case of degree distribution, this means that the expected node degree grows as the graph accumulates more nodes.

5.2 Evolving Degree Distribution

Graphs also exist with degree distribution $\gamma > 2$ which can densify. Now we allow the degree distribution to change over time. In fact, the degree distribution has to flatten over time to accumulate more mass in the tail as more nodes are added to allow for densification. This is what we explore next.

In the previous section, we assumed that the exponent γ of the power-law degree distribution remains constant over time, and then found the range for power-law degree exponent γ where it leads to densification. Now, we assume densification power law with exponent a, allow degree distribution to change over time, and ask How should the power-law degree exponent γ change over time to allow for densification? We show the following result.

THEOREM 5.2. *Given a time evolving graph on n nodes that evolves according to densification power law with exponent $a > 1$ and has a power-law degree distribution with exponent $\gamma_n > 2$, then the degree exponent γ_n evolves with the number of nodes n as*

$$\gamma_n = \frac{4n^{a-1} - 1}{2n^{a-1} - 1}. \tag{7}$$

PROOF. An undirected graph G on n nodes has $e = \frac{1}{2}n\bar{d}$ edges, where $\bar{d}$ is the average degree in graph G. Then the densification power law exponent a is

$$a = \frac{\log(e)}{\log(n)} = \frac{\log(n) + \log(\bar{d}) - \log(2)}{\log(n)}. \tag{8}$$

In a graph with power-law degree distribution, $p(x) = x^{-\gamma}$ with exponent $\gamma > 2$, the average degree $\bar{d}$ is

$$\bar{d} \approx \int_1^\infty x p(x)\ \mathrm{d}x = c \int_1^\infty x^{-\gamma+1}\ \mathrm{d}x = \frac{c}{2-\gamma} x^{-\gamma+2} \Big|_1^\infty = \frac{\gamma - 1}{\gamma - 2}. \tag{9}$$

Now, substituting $\bar{d}$ in Equation (8) with the result of Equation (9) and solving for γ, we obtain:

$$\gamma_n = \frac{4n^{a-1} - 1}{2n^{a-1} - 1}. \tag{10}$$

□

Here we found the evolution pattern that degree distribution with exponent $\gamma > 2$ has to follow in order to allow for densification. As Theorem 8 shows, the degree distribution has to flatten over time so that the expected node degree increases, which is the result of densification.

5.3 Measurements on Real Networks

Next, given the analysis from the previous section, we went back to the data and checked if graphs we analyzed before behave according to the results of Theorems 5.1 and 5.2.

First, we show an example of a graph where the evolution of the degree distribution and the densification power law exponent follow the results of Theorem 5.1. Using the email network described in Section 3.1.5, we found that the degree distribution follows a power law with exponent γ that remains constant over time.

Figure 11(a) shows the degree distribution of the the email network for the last snapshot of the network, that is, the last 2 months of the data. We create

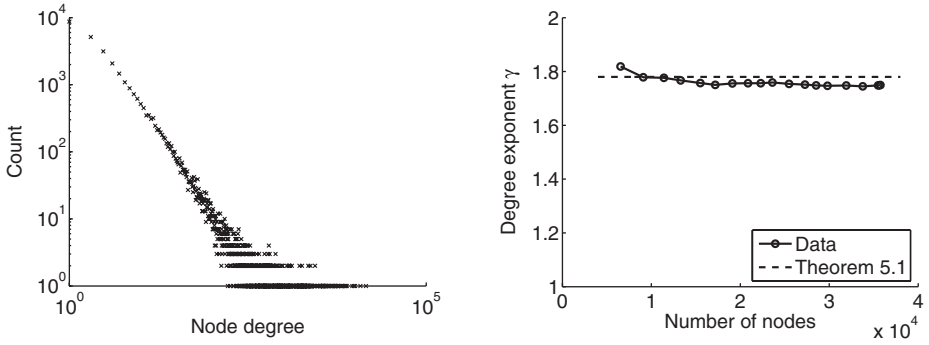

(a) Degree distribution (b) Degree exponent over time

Fig. 11. Degree distribution (a) and the degree exponent γ over time (b) for the email network. The network maintains constant slope γ of degree distribution over time. Notice that $\gamma < 2$. We observe a remarkably good agreement between the result of Theorem 5.1 (densification power law exponent $a = 1.13$), and our measurements (densification power law exponent $a = 1.11$) in Figure 2(e).

the networks by using a 2-month sliding window. We fit the power-law degree exponent γ using Maximum Likelihood Estimation (MLE), and plot its evolution over time in Figure 11(b). Notice γ remains practically constant over time which is also in agreement with observations reported in Kossinets and Watts [2006]. Also notice that the power-law degree exponent $\gamma = 1.76 < 2$. Given the degree exponent γ and using Theorem 5.1, we obtain the theoretical value of the densification power law exponent $a = 2/1.76 \approx 1.13$. The value of the DPL exponent we measured in Section 3, Figure 2(e), is $a = 1.11$, which is a remarkably good agreement. This shows that there exist graphs in the real world that densify and have decreasing diameter while maintaining constant degree exponent over time.

Last, we show an example of a temporally evolving graph that densifies and has the power-law degree exponent γ changing over time.

Figure 12(a) plots the degree distribution of the full HEP–PH citation network from Section 3.1.1. In this case, the degree distribution only follows a power law in the tail of the distribution, so we applied the following procedure. For every year y, $1992 \leq y \leq 2002$, we create a citation graph and measure the exponent of the power-law degree distribution. We apply logarithmic binning and fit the power-law degree distribution using MLE on the tail of the degree distribution starting at minimum degree 10. We plot the resulting degree exponent γ over time as a function of the size of the graph in Figure 12(b).

Using dashed lines, we also plot the degree exponent γ obtained in Theorem 5.2. Since the graph does not exhibit power-law degree distribution on the entire range and due to missing past effects, we had to appropriately scale the time axis with a manually chosen value. Regardless of the manual scaling, we think this result indicates that, for a class of temporally evolving graphs, the degree distribution flattens over time as given by Theorem 5.2. This seems to be the case for the HEP–PH citation network where the evolution of the degree exponent qualitatively follows the result of Theorem 5.2.

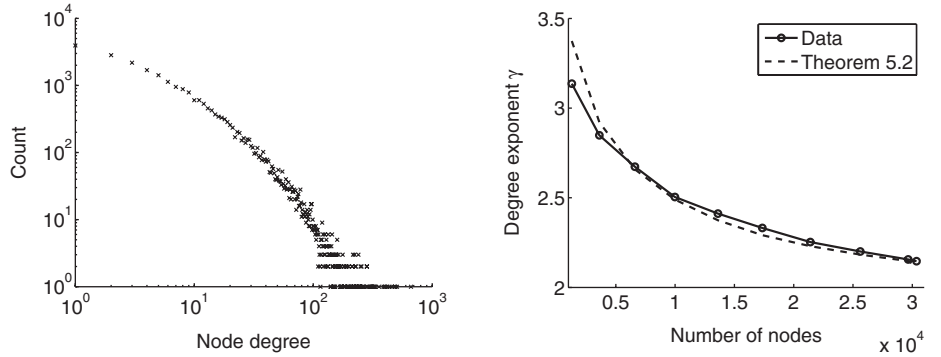

(a) Degree distribution (b) Degree exponent over time

Fig. 12. Degree distribution (a) and the degree exponent over time (b) for the HEP–PH citation network. The network follows power-law degree distribution only in the tail. Degree distribution exponent γ is decreasing over time. Notice a good agreement of degree distribution evolution (solid line) as predicted by the Theorem 5.2 (dashed line).

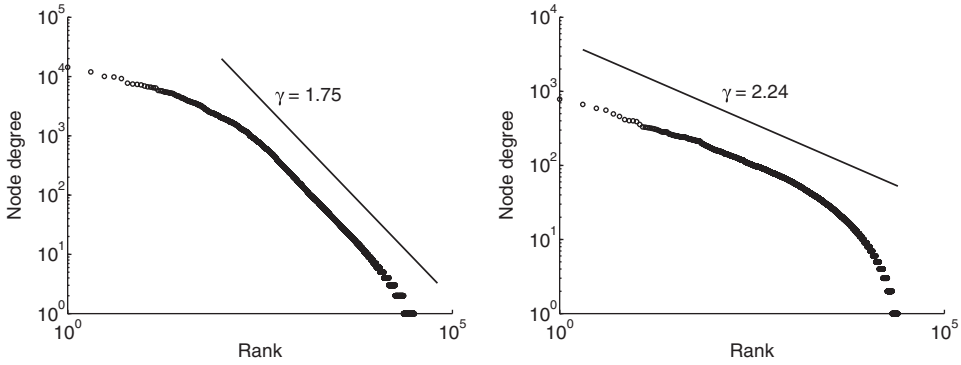

(a) Email network (b) HEP–PH citation network

Fig. 13. Rank degree plot for the degree distribution of the email and HEP–PH datasets. We use the same data as in Figures 11(a) and 12(a) but plot node degree vs. rank using the log-log scales. The solid lines present the power-law decay with exponent $\gamma = 1.75$ and $\gamma = 2.24$, respectively.

Figure 13 further investigates the degree distribution of the email and HEP–PH networks. We use the same data as in Figures 11(a) and 12(a) and plot the number of nodes of a certain degree against the rank. The solid lines present the power-law decay with exponents $\gamma = 1.75$ and $\gamma = 2.24$, respectively. The actual slope of the plotted line is $1/(\gamma - 1)$, which is the relation between the power-law exponent γ and the slope of the rank degree plot (see Adamic [2000] for more details on these relationships).

In both plots of Figure 13, we observe linearity, which suggests a power-law relationship for a part of the degree distribution. For the email network, we observe linearity in the tail and, for the HEP–PH citation network, in the first part of the distribution. These two plots show that in our two datasets, the power-law degree distribution does not hold for the entire range. However, we still observe a significant range where the power-law relationship seems to hold.

Regardless of these irregularities, there is still very good agreement of the data with the results of Theorems 5.1 and 5.2, which suggests that graphs exists that densify by maintaining constant power-law degree exponent (Theorem 5.1), and also graphs that densify by degree exponent flattening over time (Theorem 5.2).

6. CONCLUSION

Despite the enormous recent interest in large-scale network data and the range of interesting patterns identified for static snapshots of graphs (e.g., heavy-tailed distributions, small-world phenomena), there has been relatively little work on the properties of the time evolution of real graphs. This is exactly the focus of this work. The main findings and contributions follow.

—The densification power law. In contrast to the standard modeling assumption that the average out-degree remains constant over time, we discover that real graphs have out-degrees that grow over time, following a natural pattern (Equation (1)).
—Shrinking diameters. Our experiments also show that the standard assumption of slowly growing diameters does not hold in a range of real networks, rather the diameter may actually exhibit a gradual decrease as the network grows.
—We show that our Community Guided Attachment model leads to the densification power law and that it needs only one parameter to achieve it.
—We give the Forest Fire Model, based on only two parameters, which is able to capture patterns observed both in previous work and in the current study: heavy-tailed in- and out-degrees, the densification power law, and a shrinking diameter.
—We notice that the Forest Fire Model exhibits a sharp transition between sparse graphs and graphs that are densifying. Graphs with decreasing effective diameter are generated around this transition point.
—Finally, we find a fundamental relation between the temporal evolution of the graph's power-law degree distribution and the densification power law exponent. We also observe that real datasets exhibit this type of relation.

Our work here began with an investigation of the time evolution of a set of large real-world graphs across diverse domains. It resulted in the finding that real-world graphs are becoming denser as they grow and that, in many cases, their effective diameters are decreasing. This challenges some of the dominant assumptions in recent work on random graph models, which assumes constant (or at most logarithmic) node degrees, and diameters that increase slowly in the number of nodes. Building on these findings, we have proposed a set of simple graph generation processes capable of producing graphs that exhibit densification and exhibit decreasing effective diameter.

Our results have potential relevance in multiple settings, including what if scenarios, forecasting of future parameters of computer and social networks, anomaly detection on monitored graphs, designing graph sampling algorithms, and in realistic graph generators.

ACKNOWLEDGMENTS

We thank Panayiotis Tsaparas of HIIT for helpful comments, Michalis Faloutsos and George Siganos of UCR for help with the data and for early discussions on the Autonomous System dataset, and Sergey Dorogovtsev and Alexei Vazquez for pointing us to references.

REFERENCES

ABELLO, J. 2004. Hierarchical graph maps. *Comput. Graph. 28*, 3, 345–359.

ABELLO, J., BUCHSBAUM, A. L., AND WESTBROOK, J. 1998. A functional approach to external graph algorithms. In *Proceedings of the 6th Annual European Symposium on Algorithms*. Springer-Verlag, 332–343.

ABELLO, J., PARDALOS, P. M., AND RESENDE, M. G. C. 2002. *Handbook of Massive Data Sets*. Kluwer Academic Publishing.

ADAMIC, L. A. 2000. Zipf, power-law, pareto—a ranking tutorial. `http://www.hpl.hp.com/research/idl/papers/ranking`.

ALBERT, R. AND BARABASI, A.-L. 1999. Emergence of scaling in random networks. *Science*. 509–512.

ALBERT, R., JEONG, H., AND BARABASI, A.-L. 1999. Diameter of the World-Wide Web. *Nature 401*, 130–131.

ALDERSON, D., DOYLE, J. C., LI, L., AND WILLINGER, W. 2005. Towards a theory of scale-free graphs: Definition, properties, and implications. *Internet Math. 2*, 4.

BI, Z., FALOUTSOS, C., AND KORN, F. 2001. The dgx distribution for mining massive, skewed data. In *Proceedings of Knowledge Discovery and Data Mining (KDD)*. 17–26.

BOLLOBAS, B. AND RIORDAN, O. 2004. The diameter of a scale-free random graph. *Combinatorica 24*, 1, 5–34.

BRODER, A., KUMAR, R., MAGHOUL, F., RAGHAVAN, P., RAJAGOPALAN, S., STATA, R., TOMKINS, A., AND WIENER, J. 2000a. Graph structure in the Web. In *Proceedings of the 9th International World Wide Web Conference on Computer Networks: The International Journal of Computer and Telecommunications Netowrking*. North-Holland Publishing Co., Amsterdam, The Netherlands, 309–320.

BRODER, A., KUMAR, R., MAGHOUL, F., RAGHAVAN, P., RAJAGOPALAN, S., STATA, R., TOMKINS, A., AND WIENER, J. 2000b. Graph structure in the web: experiments and models. In *Proceedings of World Wide Web Conference*.

CHAKRABARTI, D. AND FALOUTSOS, C. 2006. Graph mining: Laws, generators, and algorithms. *ACM Comput. Sur. 38*, 1.

CHAKRABARTI, D., ZHAN, Y., AND FALOUTSOS, C. 2004. R-mat: A recursive model for graph mining. In *Proceedings of the SIAM Conference on Data Mining (SDM)*.

CHUNG, F. AND LU, L. 2002. The average distances in random graphs with given expected degrees. *Proceedings of the National Academy of Sciences 99*, 25, 15879–15882.

COOPER, C. AND FRIEZE, A. 2003. A general model of web graphs. *Random Struct. Algo. 22*, 3, 311–335.

DOROGOVTSEV, S. AND MENDES, J. 2001a. Effect of the accelerated growth of communications networks on their structure. *Phys. Rev. E 63*, 025101.

DOROGOVTSEV, S. AND MENDES, J. 2001b. Language as an evolving word web. *Proceedings of the Royal Society of London B 268*, 2603.

DOROGOVTSEV, S. AND MENDES, J. 2002. Accelerated growth of networks. In *Handbook of Graphs and Networks: From the Genome to the Internet, S. Bornholdt and H.G. Schuster*. Eds. Wiley-VCH, Berlin, Germany.

DOROGOVTSEV, S. AND MENDES, J. 2003. *Evolution of Networks: From Biological Nets to the Internet and WWW*. Oxford University Press, Oxford, UK.

FALOUTSOS, M., FALOUTSOS, P., AND FALOUTSOS, C. 1999. On power-law relationships of the Internet topology. In *SIGCOMM*. 251–262.

GEHRKE, J., GINSPARG, P., AND KLEINBERG, J. M. 2003. Overview of the 2003 kdd cup. *SIGKDD Explora. 5*, 2, 149–151.

HALL, B. H., JAFFE, A. B., AND TRAJTENBERG, M. 2001. The nber patent citation data file: Lessons, insights and methodological tools. NBER Working Papers 8498, National Bureau of Economic Research, Inc. (Oct.)

HUBERMAN, B. A. AND ADAMIC, L. A. 1999. Growth dynamics of the world-wide web. *Nature 399*, 131.

KATZ, J. S. 1999. The self-similar science system. *Resear. Policy 28*, 501–517.

KATZ, J. S. 2005. Scale independent bibliometric indicators. *Measure.: Interdisciplin. Resea. Perspect. 3*, 24–28.

KLEINBERG, J. M. 2002. Small-world phenomena and the dynamics of information. In *Advances in Neural Information Processing Systems 14*.

KLEINBERG, J. M., KUMAR, R., RAGHAVAN, P., RAJAGOPALAN, S., AND TOMKINS, A. 1999. The Web as a graph: Measurements, models, and methods. In *Proceedings of the International Conference on Combinatorics and Computing*. 1–17.

KOSSINETS, G. AND WATTS, D. J. 2006. Empirical analysis of an evolving social network. *Science 311*, 88–90.

KRAPIVSKY, P. L. AND REDNER, S. 2001. Organization of growing random networks. *Phys. Rev. E 63*, 066123.

KRAPIVSKY, P. L. AND REDNER, S. 2005. Network growth by copying. *Phys. Rev. E 71*, 036118.

KUMAR, R., RAGHAVAN, P., RAJAGOPALAN, S., SIVAKUMAR, D., TOMKINS, A., AND UPFAL, E. 2000. Stochastic models for the web graph. In *Proceedings of the 41st IEEE Symposium on Foundations of Computer Science*.

KUMAR, R., RAGHAVAN, P., RAJAGOPALAN, S., AND TOMKINS, A. 1999. Trawling the Web for emerging cyber-communities. In *Proceedings of the 8th International World Wide Web Conference*.

LESKOVEC, J., ADAMIC, L., AND HUBERMAN, B. 2006. The dynamics of viral marketing. *ACM Conference on Electronic Commerce*.

LESKOVEC, J., CHAKRABARTI, D., KLEINBERG, J. M., AND FALOUTSOS, C. 2005. Realistic, mathematically tractable graph generation and evolution, using kronecker multiplication. In *Proceedings of the European International Conference on Principles and Practice of Knowledge Discovery in Databases (PKDD'05)*. 133–145.

LESKOVEC, J. AND FALOUTSOS, C. 2006. Sampling from large graphs. In *Proceedings of the 12th ACM SIGKDD International Conference on Knowledge Discovery and Data Mining (KDD'06)*. ACM Press, New York, NY, USA, 631–636.

LESKOVEC, J., KLEINBERG, J., AND FALOUTSOS, C. 2005. Graphs over time: densification laws, shrinking diameters and possible explanations. In *Proceedings of the International Conference on Knowledge Discovery and Data Mining (KDD'05)*. Chicago, IL.

MENCZER, F. 2002. Growing and navigating the small world web by local content. *Proceedings of the National Academy of Sciences 99*, 22, 14014–14019.

MILGRAM, S. 1967. The small-world problem. *Psycholo. Today 2*, 60–67.

MITZENMACHER, M. 2004. A brief history of generative models for power law and lognormal distributions. *Internet Math. 1*, 2, 226–251.

NEWMAN, M. E. J. 2003. The structure and function of complex networks. *SIAM Review 45*, 167–256.

NEWMAN, M. E. J. 2005. Power laws, pareto distributions and zipf's law. *Contemp. Phys. 46*, 323–351.

NTOULAS, A., CHO, J., AND OLSTON, C. 2004. What's new on the web? the evolution of the web from a search engine perspective. In *World Wide Web Conference*. New York, 1–12.

OREGON. 1997. University of Oregon route views project. online data and reports. `http://www.routeviews.org`.

PALMER, C. R., GIBBONS, P. B., AND FALOUTSOS, C. 2002. Anf: A fast and scalable tool for data mining in massive graphs. In *SIGKDD*. Edmonton, AB, Canada.

REDNER, S. 2004. Citation statistics from more than a century of physical review. Tech. rep. physics/0407137, arXiv.

SCHROEDER, M. 1991. *Fractals, Chaos, Power Laws: Minutes from an Infinite Paradise*. W.H. Freeman and Company, New York, NY.

TAURO, S. L., PALMER, C., SIGANOS, G., AND FALOUTSOS, M. 2001. A simple conceptual model for the internet topology. In *Global Internet*. San Antonio, TX.

VAZQUEZ, A. 2001. Disordered networks generated by recursive searches. *Europhy. Lett. 54*, 4, 430–435.

VAZQUEZ, A. 2003. Growing networks with local rules: Preferential attachment, clustering hierarchy and degree correlations. *Physical Review E 67*, 056104.

WATTS, D. J., DODDS, P. S., AND NEWMAN, M. E. J. 1998. Collective dynamics of 'small-world' networks. *Nature 393*, 440–442.

WATTS, D. J., DODDS, P. S., AND NEWMAN, M. E. J. 2002. Identity and search in social networks. *Science 296*, 1302–1305.

Received March 2006; revised October 2006; accepted December 2006